FERMILAB-PUB-19-172-T

Lattice QCD and Neutrino-Nucleus Scattering

Andreas S. Kronfeld,[1,*] David G. Richards,[2,†] William Detmold,[3] Rajan Gupta,[4] Huey-Wen Lin,[5] Keh-Fei Liu,[6] Aaron S. Meyer,[7] Raza Sufian,[2] and Sergey Syritsin[8]

(USQCD Collaboration)

[1] *Theoretical Physics Department, Fermi National Accelerator Laboratory, Batavia, IL 60510*
[2] *Theory Center, Thomas Jefferson National Accelerator Facility, Newport News, VA 23606*
[3] *Center for Theoretical Physics, Massachusetts Institute of Technology, Cambridge, MA 02139*
[4] *Group T-2, Los Alamos National Laboratory, Los Alamos, NM 87545*
[5] *Department of Physics and Astronomy, Michigan State University, East Lansing, MI 48824*
[6] *Department of Physics and Astronomy, University of Kentucky, Lexington, KY 40508*
[7] *Physics Department, Brookhaven National Laboratory, Upton, NY 11973*
[8] *Department of Physics and Astronomy, Stony Brook University, Stony Brook, NY 11794*

(Dated: April 23, 2019)

Abstract

This document is one of a series of whitepapers from the USQCD collaboration. Here, we discuss opportunities for lattice QCD in neutrino-oscillation physics, which inevitably entails nucleon and nuclear structure. In addition to discussing pertinent lattice-QCD calculations of nucleon and nuclear matrix elements, the interplay with models of nuclei is discussed. This program of lattice-QCD calculations is relevant to current and upcoming neutrino experiments, becoming increasingly important on the timescale of LBNF/DUNE and HyperK.

This manuscript has been authored by Fermi Research Alliance, LLC under Contract No. DE-AC02-07CH11359 with the U.S. Department of Energy, Office of Science, Office of High Energy Physics.

* Editor, ask@fnal.gov
† Editor, dgr@jlab.org

EXECUTIVE SUMMARY

In 2018, the USQCD collaborations Executive Committee organized several subcommittees to recognize future opportunities and formulate possible goals for lattice field theory calculations in several physics areas. The conclusions of these studies, along with community input, are presented in seven whitepapers [1–6]. This whitepaper covers the role of lattice QCD in neutrino-nucleus scattering, motivated principally by neutrino oscillations.

Neutrino-nucleus scattering experiments provide an abundance of information on neutrino masses and flavor mixing, on nucleon and nuclear structure, and on non-standard interactions between neutrinos and ordinary matter. To interpret these experiments cleanly, the key problem is to reconstruct the incident neutrino energy. The nuclear remnant is not, in these experiments, detected. It is therefore impossible to reconstruct the neutrino energy without modeling the nucleus in some way. This problem is complex, because it spans a range of energies—from hundreds of keV to a few GeV—that probe all aspects of the target nucleus.

The presence of many energy scales implies that a variety of theoretical techniques must work in concert. A convenient, organizational framework is nuclear many-body theory, which takes nucleonic properties as inputs. In this whitepaper, we discuss how these nucleonic properties can be obtained directly from the QCD Lagrangian using numerical simulations of lattice gauge theory. Although lattice QCD cannot settle every question in neutrino-nucleus scattering, it is reasonable to demand that our understanding of these processes be consistent with QCD. In many cases, the most straightforward route to the needed QCD knowledge is lattice QCD.

In this whitepaper, we discuss several calculations that should, as they mature, be incorporated into nuclear theory and neutrino event generators. A very important and very feasible example is the axial form factor of the nucleon. Lattice QCD has a notable history of calculating this and related observables, and calculations with full control of the systematic uncertainties are now coming of age. Here, "full control of systematic uncertainties" implies that a complete error budget is provided. The axial form factor is relatively straightforward: completely analogous calculations of vector form factors are possible with the same (indeed, overlapping) computational effort. The vector form factors have been measured in electron-proton and -neutron scattering, so an apt crosscheck is close at hand. Experience from form factors in meson physics suggests a simple, model-independent way to transmit the output of lattice QCD to event generators and, thus, analysis of experimental data.

Form factors of nucleons are only the beginning. Future oscillation experiments span beam energies such that computationally more demanding information is required. Just at the nucleon level, transition form factors to multibody final states are needed. For an inclusive data set, the object of interest is the nuclear hadron tensor, which can be obtained by combining the nucleonic hadron tensor from lattice QCD with a nuclear spectral function. In the deep inelastic region, new ways of computing parton distribution functions in lattice QCD are an exciting development. A further emerging component of lattice QCD consists of calculations of the properties of small nuclei—up to ^{4}He today and to ^{6}Li with exascale computing—can be used to test nuclear many-body theory and provide information via chiral effective theories to pin down the nuclear physics.

Lattice-QCD calculations with nucleon and nuclei are more challenging than the corresponding ones for mesons, because of unavoidable technical challenges that increase with the number of quark lines. Consequently, to perform the requisite calculations, improvements in methodology, algorithms, and software will be essential. Even assuming continuing

ingenuity on those fronts, much of the work will require exascale computing resources. As in the past, a combination of high-capability and high-capacity computing will be needed. The former is needed for timely solution of mature problems, while the latter is necessary for developing feasible techniques for the challenging calculations, before making the jump to supercomputer centers.

I. INTRODUCTION

Along with the first observation of the Higgs boson and the mounting evidence for dark matter, the discovery that neutrinos change flavor is one of the major advances in particle physics over the past twenty-five years. The discovery hinged on studies of neutrinos produced at the upper edge of the earth's atmosphere [7] and also explained a deficit in electron neutrinos from the sun [8]. These findings prompted an accelerator-based experimental program in Europe, Japan, and the United States, to make more accurate measurements of, for example, the squared mass differences. The increase in precision and sensitivity expected in future experiments raises the question whether the theoretical description of the relevant experiments must be further refined to exploit the new measurements to the fullest. In particular, as future, ambitious, long-baseline neutrino-oscillation experiments such as LBNF/DUNE [9] and HyperK [10] have come into focus, the quantification of uncertainties from the hadronic and nuclear physics of the detectors have become increasingly relevant. To this end, the lattice-QCD community has identified a set of feasible calculations that will be of special relevance. This program is described in this whitepaper.

An important goal of the experimental neutrino-physics program is to test the three-neutrino paradigm of the Standard Model. In this context, the Standard Model must be extended to allow for lepton flavor change. The simplest choice consistent with the standard gauge symmetries is to introduce a set of right-handed neutrino fields. Then lepton-flavor mixing and neutrino masses arise in the same way as in the quark sector, namely through Yukawa couplings to the Higgs field with a nonvanishing vacuum expectation value. To couple to the Higgs and left-handed-lepton doublets, the right-handed neutrino fields have to be gauge singlets. But then no symmetry principle forbids a mass term connecting neutrinos to themselves (i.e., of the kind first noted by Majorana [11]), in contrast to the Higgs-generated Dirac mass term, which connects neutrino to antineutrino. The lack of direct evidence for right-handed neutrinos suggests that in this scenario the Majorana mass M might be very large. If one supposes that the neutrino Yukawa couplings are not much different from light quarks or charged leptons, the propagating neutrinos have mass close to M and to $m_\nu \approx y^2 v^2/2M$, where y is a Yukawa coupling and v is the vacuum expectation value of the Higgs field. This mass hierarchy, known as the see-saw mechanism, provides a possible explanation of the tiny size of neutrino masses [12]. For example, if M is a grand-unified mass scale around 10^{15} GeV, then $m_\nu \lesssim 0.03$ eV (for $y \lesssim 1$).

This theoretical framework means that the three-neutrino paradigm can be tested by measuring the neutrino mass-squared differences and the mixing angles and CP violating phases of the Pontecorvo-Maki-Nakagawa-Sakata (PMNS) mixing matrix [13]. Like the Cabibbo-Kobayashi-Maskawa (CKM) quark-mixing matrix [14], the PMNS has three mixing angles. If the Majorana mass term appears, the PMNS matrix has three CP-violating phases instead of one as in the CKM matrix. The mixing angles and the CKM-like CP-violating phase can be measured in oscillation experiments, while the extra phases and the Majorana nature of neutrinos can be probed via the neutrinoless double-beta ($0\nu\beta\beta$) decay of certain nuclei. For lattice-QCD calculations relevant to $0\nu\beta\beta$, see the companion whitepaper "The Role of Lattice QCD in Searches for Violations of Fundamental Symmetries and Signals for New Physics" [3]; here, the focus is on lattice-QCD research that will impact the oscillation experiments.

Oscillation experiments measure the energy spectrum of a neutrino beam after it has travelled a certain baseline distance. Unfortunately, neutrino beams have a wide energy

spectrum, as shown in Fig. 1, so the center-of-mass energy of a collision is not known. In contrast, quark-flavor experiments, for which lattice QCD has been crucial, study decays of strange, charmed, or b-flavored hadrons of precisely known mass. Here, the energy of the incident neutrino must be inferred from measurements of the final state. The targets in neutrino experiments are medium- to large-sized nuclei, such as ^{12}C, ^{16}O, or ^{40}Ar, the remnants of which are not, in practice, be detected. That means that the mapping between final-state measurements and the initial energy inevitably requires theoretical knowledge of the neutrino interaction with the struck nucleus.

Consistency with QCD is a clearly desirable characteristic of nuclear models used to deduce the connection between final and initial states. Thus, it makes sense to incorporate lattice QCD as soon as results with full, reliable error budgets are available. As discussed in more detail in Ref. [16], the nuclear models rely in part on properties of the nucleon as inputs. Many of these quantities can be calculated in lattice QCD in the near term, with the precision depending on the quantity. Of course, single-nucleon calculations are not in themselves enough. Calculations of the properties of multi-nucleon systems must be developed concurrently and, once mature, also incorporated into the nuclear modeling.

The theory behind neutrino-nucleus collisions is complex because it spans a range of energies that probe all aspects of the target nucleus. Nuclear excitation energies are, typically, dozens of keV, while the average binding energy is 8.6 MeV (in ^{40}Ar), and the typical Fermi motion of a nucleon is around 250 MeV. In the regime relevant to oscillation experiments, the energy transfer to the nucleus ranges between ∼200 MeV and the neutrino energy itself, although much of transferred energy is carried off by nucleons and pions, rather than the nuclear remnant. Thus, it is a challenge to arrive at a comprehensive approach to the entire problem. Most approaches start with nuclear many-body theories, in which the nucleus is described by a nuclear wave function of a collection of interacting nucleons; see, for example, Ref. [17, 18]. It is at this point in the analysis that nucleon-level matrix elements enter. One should bear in mind, however, that single-nucleon physics is not enough: multi-body

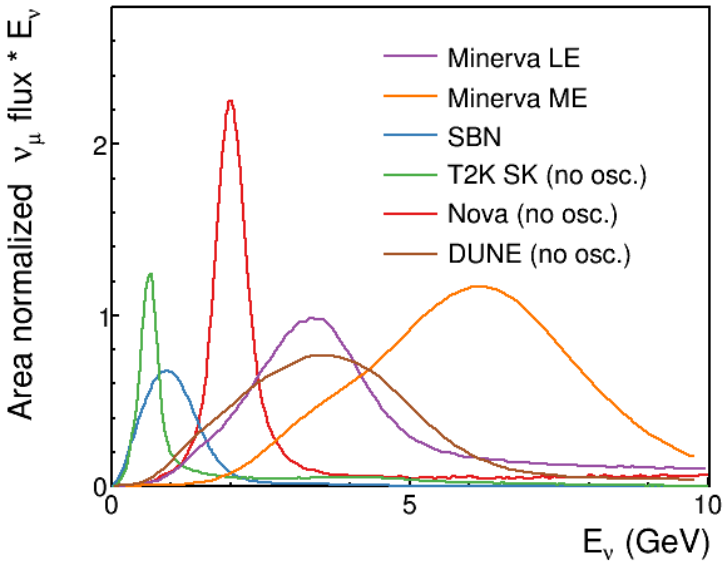

FIG. 1. Energy spectrum of the neutrino beam for several experiments. In particular, most of DUNE's beam lies in the range 1 GeV $< E_\mu <$ 7 GeV. Courtesy Laura Fields [15].

effects are needed for scattering events that knock out two (or more) nucleons. Even in nuclear spectroscopy, three-body potentials improve the agreement with observed nuclear levels [18–20]. Often these calculations use phenomenological potentials, but effective field theory (EFT) offers a direct connection to QCD [21–24]. Chiral EFTs are, however, limited to a kinematic range where the momenta are small relative to the chiral symmetry breaking scale $\Lambda_\chi \sim 700$ MeV. Even then, the reliability of the application of nuclear EFT to large atomic number systems, such as argon, requires significant development, testing, and, eventually, verification. These issues are further intertwined with the constraints of how event generators [25–29] and detector simulations are implemented. Inconsistencies arise in the current approach where, for example, the axial form factor of the nucleon is extracted from νA scattering data assuming one nuclear model and then used in event generators employing another.

A central goal of nuclear theory in this arena should therefore be to define a path forward that allows for a quantified nuclear uncertainty to be presented for experiments such as DUNE and HyperK. Achieving this is a challenging task and will require input and constraints from lattice QCD in order for it to be successful. In addition to the single- and few-nucleon amplitudes noted above, it will be valuable to compute directly the properties of small nuclei. At present, calculations involving nuclei up to ^{4}He are possible. In addition to being interesting in their own right, such lattice-QCD calculations of few nucleon systems can be used to constrain low energy constants (LECs) in the EFTs. This approach has already been applied to static quantities, such as magnetic moments. A next step will be to work with matrix elements of electroweak currents, to build up effects associated with two- and higher-body contributions, as well as more complex contributions such as pion production. In combination with experimental constraints from eA scattering, and neutrino scattering on light nuclear targets,[1] it is hoped a robust uncertainty can be determined.

To study neutrino oscillations, we are interested in the processes

$$\nu_\ell A \to \ell^- X, \qquad \bar{\nu}_\ell A \to \ell^+ X, \tag{1.1}$$

where A denotes the nucleus and X the combination of all final-state hadrons including the remnant of the nucleus. The charged weak current responsible for these interactions has the well-known $V-A$ structure. Properties of the vector current can be inferred from electromagnetic scattering, up to isospin corrections (which are negligible for the needed precision; see Sec. IV). On the other hand, because the weak charge of the proton is so small, $Q_{\rm w}^p = 0.0719 \pm 0.0045$ [31], at the energies of interest, only neutron-neutrino (and proton-antineutrino) scattering is sensitive to the axial current. These circumstances offer the possibility of testing lattice-QCD methodology with the vector current before relying on it for the axial current.

The quantity needed to describe the strong-interaction side of the scattering depends on the energy transferred. At the lowest energies, the only possibility is coherent elastic scattering via the weak neutral current, with $X = A$ [32, 33]. Coherent neutrino-nucleus interactions have recently been observed for the first time [34]. As the energy increases slightly, the excitation spectrum of A is traced out: $X = A^*$. The needed quantities are matrix elements between different nuclear levels. In lattice QCD, one would have to simulate the whole nucleus directly, which is currently feasible only for nuclei much smaller than those in the cesium-iodide detector of Ref. [34].

[1] Indeed, recent discussions of future experiments with deuterium or hydrogen targets [30] hinge on noting the utility of nucleon-level amplitudes in nuclear many-body theory.

At high enough (but still low) energy, a single nucleon can be knocked out. At its heart, the scattering is

$$\nu_\ell n \to l^- p, \qquad \bar{\nu}_\ell p \to l^+ n, \tag{1.2}$$

with the initial and final-state nucleons in the nuclear environment. Such scattering off of a constituent in a bound-state without extra particles is known as quasielastic. Then nuclear many-body theory requires single-nucleon matrix elements of the form $\langle p(p')|J_\nu|n(p)\rangle$, between a neutron of momentum p and a proton of momentum p' (or the $p \to n$ counterpart for antineutrino beams). These matrix elements are straightforward to calculate in lattice QCD; see Sec. II. If pions can be produced, the final state can be a $\Delta(1232)$ resonance, an excited nucleon N^*, or a two-body state $N\pi$. In the experiment, these all end up as $N\pi$ so their amplitudes interfere. In fact, lattice QCD can provide not only the associated transition matrix elements, in the idealization of the resonance as a stable particle (e.g., $\langle\Delta^+|J_\nu|n\rangle$), but also enough information to describe the full multi-hadron nature of the final state (at least up to further inelasticities); see Sec. III. The quasielastic and resonance regions overlap, because the kinetic energy of Fermi motion is a bit larger than the pion mass. This overlap is illustrated with experimental data in Fig. 2. Another contribution in this region arises from many-body nuclear dynamics, for example, when the probe interacts with pairs of correlated nucleons. This contribution is described by "two-body currents" (see Refs. [36, 37] and references therein). Now a further set of matrix elements is needed, namely of the form $\langle NN|J_\nu|NN\rangle$. Note that in QCD language, the same current is employed just for two-body initial and final states.

Once the energy is high enough to produce several pions, it is not possible to enumerate every final-state hadron. In this case, however, lattice QCD can be used to compute nucleon and nuclear structure functions. In high-energy physics, structure functions are most familiar in deep-inelastic scattering, where the operator-product expansion (OPE) can be used. Lattice-QCD calculations can be used to determine the moments of the parton distribution functions (PDFs) that enter in the deep-inelastic region, and indeed extraction of the full dependence of PDFs on the longitudinal momentum fraction, x, is becoming possible [38]. Moreover, the definition of structure functions is very general. Lattice QCD may be an

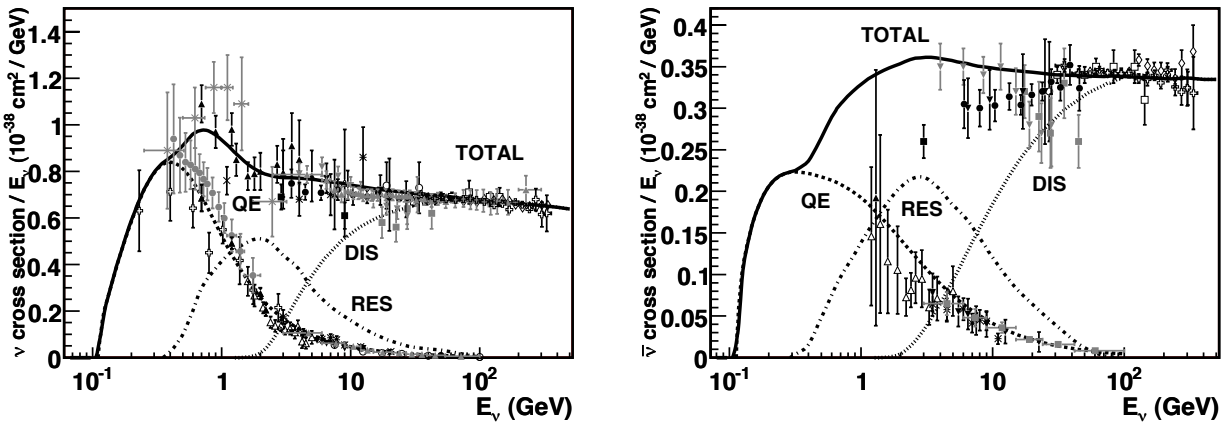

FIG. 2. Cross sections vs neutrino energy (left) or antineutrino energy (right), showing the relative contributions of the underlying processes quasielastic scattering, resonance production, and deep-inelastic scattering [35].

ideal way to compute them in the so-called shallow-inelastic region with energy above the resonance region but insufficient for the OPE; see Sec. III.

In summary, then, the goals for lattice QCD for neutrino oscillation physics are to calculate matrix elements of the form

$$\langle f|J_\nu|i\rangle, \qquad \langle f|J_\mu^\dagger J_\nu|i\rangle, \qquad \langle f|\mathcal{O}|i\rangle, \tag{1.3}$$

where the initial and final states are single nucleons, two nucleons, nucleons with a pion (including resonances), or small nuclei. In the last case, $\mathcal{O}$ denotes an operator appearing in the OPE, or a bilocal, spatially-separated operator arising in the calculation of PDFs. The lattice-QCD calculations of these and related matrix elements have a long history, motivated principally by the desire to understand nucleon and nuclear structure. For a broad survey, see our companion whitepaper "Hadrons and Nuclei" [4].

Recall that lattice QCD calculates hadronic correlation functions, which contain information about the masses and matrix elements of interest; the information is extracted by fitting the behavior of the correlation functions in (Euclidean) time. Several technical difficulties make baryon calculations more difficult than the corresponding calculations for mesons. First, statistical errors on baryon correlation functions are larger and more poorly behaved in time [41–43]. Second, it has proven more difficult, in practice, to disentangle matrix elements of the ground-state baryons from that of their excitations [44]. Last, the dependence of baryon properties on the light quark mass (used in the simulation) is less well described by the low-energy EFT of pions and baryons. All these difficulties can be addressed with more computing. The signal-to-noise problem can clearly be attacked with higher statistics. It can also be mitigated by choosing more sophisticated operators to create and annihilate baryon states; this method is also the way to better filter out the excited states. Finally, more computing also enables simulations with lighter and even physical quark masses [39, 40, 45].

The rest of this whitepaper is organized as follows. In Sec. II, we discuss calculations that are relatively straightforward. These include nucleon form factors, which are needed to describe quasielastic scattering, and moments of PDFs, which are needed in the deep-inelastic region. We discuss the form factors in considerable detail, because the time to incorporate these results into event generators is soon or, arguably, now. In particular, having the correct slopes for the form factors is crucial to gaining quantitative control of the cross section. More challenging calculations are covered in Sec. III. This class of problems is large and varied: transitions to resonances and multibody states, calculations for shallow- and deep-inelastic scattering, and the vector and axial matrix elements of small nuclei. Section IV turns to calculations that are far enough beyond that state of the art that new ideas or computing facilities greater than exascale are needed. Foreseeable computing needs are covered in Sec. V, noting the separate needs for both capability and capacity computing.

II. STRAIGHTFORWARD CALCULATIONS

The most straightforward matrix elements to calculate are those with one stable hadron in the initial state, and one or none in the final state. Here we focus on the matrix elements of electroweak currents, $\langle N|J_\mu|N\rangle$, which directly enter neutrino-nucleon scattering, and matrix elements of local operators, $\langle N|\mathcal{O}|N\rangle$, where $\mathcal{O}$ appears in the operator-product expansion of two J currents, which arise in the analysis of deep-inelastic scattering.

A. Nucleon form factors

As discussed in Sec. I, neutrino-nucleon scattering, Eq. (1.2) is a key process even though the target is a nucleus. The $V-A$ charged current of interest is $J^+_\mu = \bar{u}\gamma_\mu(1-\gamma_5)d$. The matrix element for $n \to p$ can be decomposed into Lorentz covariant combinations of momentum and spin, multiplied by form factors [46]:

$$\langle p(p')|J^+_\mu|n(p)\rangle = \bar{u}^{(p)}(p')\left[\gamma_\mu F_1^{\rm CC}(q^2) + i\sigma_{\mu\nu}\frac{q^\nu}{2M_N}F_2^{\rm CC}(q^2) + \frac{q_\mu}{M_N}F_S^{\rm CC}(q^2)\right.$$
$$\left. + \gamma_\mu\gamma_5 F_A^{\rm CC}(q^2) + \gamma_5\frac{q_\mu}{M_N}F_P^{\rm CC}(q^2) + \gamma_5\frac{(p'+p)_\mu}{M_N}F_T^{\rm CC}(q^2)\right]u^{(n)}(p), \quad (2.1)$$

where $M_N = (M_p + M_n)/2$, $q = p' - p$ and $\bar{u}$ and u are associated spinor factors. $F_1^{\rm CC}(q^2)$, $F_2^{\rm CC}(q^2)$, $F_A^{\rm CC}(q^2)$, and $F_P^{\rm CC}(q^2)$ are known as the Dirac, Pauli, axial, and induced pseudoscalar form factors, respectively. The induced scalar and tensor form factors, $F_S^{\rm CC}(q^2)$ and $F_T^{\rm CC}(q^2)$, are suppressed by G parity violation; they are known as second-class currents [47]. For neutral-current processes, additional form factors $F_i^{{\rm EM},N}$ and $F_i^{{\rm NC},N}$ are needed: the charged-currents are all isovector, but the neutral currents contain an isoscalar contribution as well. Here, N denotes either a proton p or neutron n.

Because the up- and down-quark masses are so similar, isospin violation can be neglected and, thus, the charged-current form factors of the vector current (i.e., Dirac and Pauli) can be related to their electromagnetic counterparts, up to small corrections from isospin violation. The Dirac and Pauli form factors are usually re-expressed as electric, $G_E(q^2) = F_1(q^2) + q^2F_2(q^2)/(M_n+M_p)^2$, and magnetic, $G_M(q^2) = F_1(q^2) + F_2(q^2)$, form factors (even for CC and NC). Expressions relating the differential neutrino-nucleon cross section to the form factors can be found, for example, in Refs. [35, 48].

Most neutrino scattering experiments are performed in a kinematic region of a few GeV, so tracing out the full q^2 dependence is possible and desirable (see below). Below 1 GeV it is convenient to focus attention on the intercepts $F_i(0)$ and (conventionally normalized) slopes

$$r_E^2 \equiv 6\left.\frac{dG_E}{dq^2}\right|_{q^2=0}, \quad r_M^2 \equiv \frac{6}{G_M(0)}\left.\frac{dG_M}{dq^2}\right|_{q^2=0}, \quad r_i^2 \equiv \frac{6}{F_i(0)}\left.\frac{dF_i}{dq^2}\right|_{q^2=0}, \quad (2.2)$$

for $i \in \{A, S, T, P\}$. The quantities r_i are usually called "radii", although the neutron's r_E^2 is negative.

A precise knowledge of the charged-current versions of these quantities is essential for determining the neutrino-nucleon cross section. The intercepts and slopes of $G_E^{\rm CC}$ and $G_M^{\rm CC}$ are well determined from electromagnetic processes and isospin relations. Further, the intercept $F_A^{\rm CC}(0) = g_A = -1.2723(23)$ is known from neutron β decay [49]. The axial coupling g_A has been calculated in lattice QCD, although it will be some time before it can be computed with comparable precision to experiment. Nevertheless, it is an extremely important benchmark, and once the lattice-QCD precision becomes competitive with experiment, the result could clear up some puzzles surrounding neutron-decay measurements (see below).

On the other hand, the axial-charge radius-squared r_A^2 is less well known. Historically, the axial form factor has been fit to the so-called "dipole" form:

$$F_A(q^2) = \frac{g_A}{(1 - q^2/m_A^2)^2}, \quad (2.3)$$

such that $r_A^2 = 12/m_A^2$. Experiments report this "axial mass", m_A, so a comparison of reported values illustrates the current status. It has been extracted from quasielastic scattering on deuterium targets, finding (e.g.) $m_A = 1.02(3)$ GeV [50], and from pion electroproduction, finding $m_A = 1.08(4)$ GeV [51, 52]. More recent experiments find larger values: $m_A = 1.20(12)$ GeV at K2K [53], $m_A = 1.27(15)$ GeV at MINOS [54], and even $m_A = 1.35(17)$ GeV at MiniBooNE [55], in neutrino charged-current quasielastic scattering with water, iron, and mineral-oil targets, respectively. With 2p-2h corrections, however, NOMAD [56], with a Kevlar target, finds $m_A = 1.05(6)$ GeV and

MINERvA [57], with a carbon target, finds the quasielastic cross section to be compatible with $m_A = 0.99$ GeV. Note that all of these determinations of m_A assume a nuclear model for the target material, which is not the same among the various collaborations. Moreover, nuclear modeling uncertainties typically come only from varying parameters of their choice model, not from studying comparisons among different models.

The uneasy agreement of these results can be removed by switching to a model-independent parametrization of $F_A(q^2)$ [46]. For example, a reanalysis of 1980s deuterium bubble-chamber data [58] finds $\sqrt{12/r_A^2} = 1.01(24)$ GeV. These data are chosen because the nuclear model of the deuteron is under relatively good control. The main conclusion of Ref. [58] is that introducing only one free parameter with a qualitatively acceptable but conceptually incorrect shape, as in Eq. (2.3), leads to gross underestimates of the uncertainty, even when the fit quality is high.

Figure 4, from Ref. [59], shows the dependency of νn quasielastic cross section on E_ν, assuming r_A^2 is known with 20% uncertainty. As one can see, this quantity affects the both the normalization and fall-off of the cross section, which are needed, respectively, to determine the mixing angle and mass difference in an oscillation. Furthermore, a lattice-QCD calculation with 20% uncertainty (compared to 50% in Ref. [58]) is an important milestone, because then the r_A^2 uncertainty becomes subdominant, at least until other uncertainties have been reduced.

The lattice-QCD community has been pursuing the calculation of the nucleon form fac-

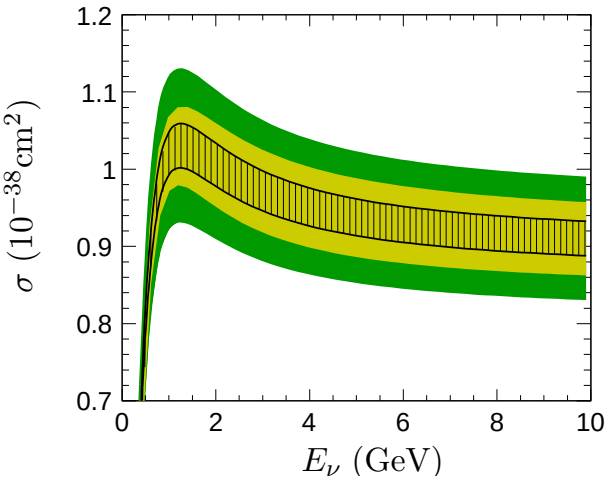

FIG. 3. Quasielastic neutrino-neutron cross section assuming current uncertainties for all crucial inputs except r_A^2, for which a 20% uncertainty is assumed. The hatched (yellow) error band stems from this putative r_A^2 (all other inputs); the green band is the sum in quadrature. From Ref. [59].

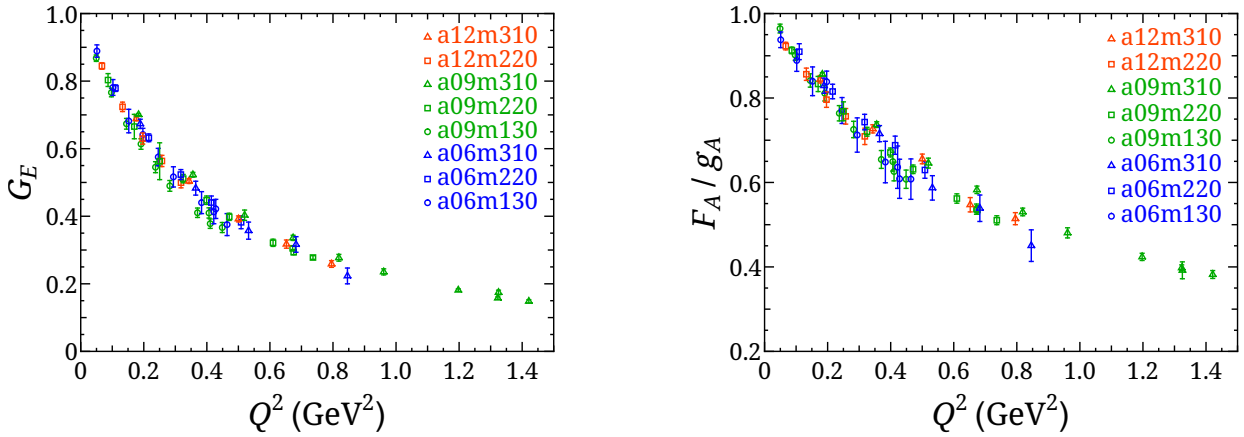

FIG. 4. Electric (left) and isovector axial (right) form factors of the nucleon vs $Q^2 = -q^2$. Data from Ref. [66, 75].

tors for a long time. A representative set of recent work can be found in Refs. [60–74] Significant improvements have been made to investigate the quark-mass, finite-volume, and finite-lattice-spacing dependence, and the effects of excited-state contamination in the correlation functions. With these technical and algorithmic advances, lattice QCD can calculate not only the isovector contribution but also the computationally more demanding isoscalar and strange-quark contributions, which are needed for neutral-current processes, discussed below.

Sample lattice-QCD calculations [66, 75] of the nucleon isovector electric and axial form factors—G_E and F_A—are shown in Fig. 4. Eight different $2+1+1$-flavor HISQ ensembles generated by the MILC collaboration [40] with lattice spacings in the range 0.06–0.12 fm and pion mass in the range 130–310 MeV are employed. In this calculation, excited-state contamination is controlled via a three-state fit. The results are in good agreement with the experimental data for the nucleon electromagnetic form factor $G_E(q^2)$ On the other hand, the axial form factor is not as steep as experimental determinations with $m_A \approx 1$ GeV [76], yet is compatible with MiniBooNE's $m_A \approx 1.35$ GeV [55]. Despite the many laudable aspects of Ref. [66], a full and robust accounting of all systematics involved in these lattice-QCD calculations has not yet been feasible. Reliable confrontation with precise experimental data for G_E—and, hence, a solid prediction of F_A—requires an increase in computational resources to overcome the technical obstacles to nucleon matrix elements, discussed in Sec. I.

The status of lattice-QCD calculations of g_A and r_A^2 is shown in Fig. 5. The left plot [77], for g_A, shows that lattice-QCD is at this time much less precise than the results from neutron β decay.[2] Note, however, that bottle and beam experiments measuring the neutron lifetime yield values of g_A that differ by 3σ. For example, a 2015 bottle measurement leads to $g_A = 1.2749(11)$ [80], while a 2013 beam measurement leads to $g_A = 1.2684(20)$ [81]. It would be interesting to know the answer from lattice QCD. The precision required depends on whether the (average of several) calculation(s) lands between the two neutron-lifetime values or outside the interval. In the latter case, at least percent-level precision is needed, which is likely to be achieved with three years (assuming sustained computing support). If

[2] The color code here is adapted from the Flavor Lattice Averaging Group [78], as specified in the Appendix of Ref. [79].

lattice QCD lands in the middle, 0.3% precision is needed. In this scenario, we would also need 1+1+1(+1)-flavor ensembles, since the isospin symmetry would play an important role at such precision; it would take 5–10 years to account for full systematics.[3]

The right plot [59], for r_A^2, shows significant problems: the analysis with the z expansion [58] debunks the uncertainty estimates of determinations predicated on the dipole form. The model independent results (red; between the horizontal lines) illustrate the best estimate of r_A^2 without such strong assumptions. One should bear in mind that the "experimental" determinations all make assumptions: without new νd and $\bar{\nu} p$ experiments [30], it seems nearly impossible to improve the situation via experiment. On the other hand, lattice gauge theory can provide an *ab initio* result from QCD. Indeed, lattice QCD is beginning to play a role, but another generation of calculations is needed before fully definitive results with uncertainties small enough to make an impact on cross section calculations are achieved.

For the full energy range of LBNF/DUNE, it will be necessary to trace out the full q^2

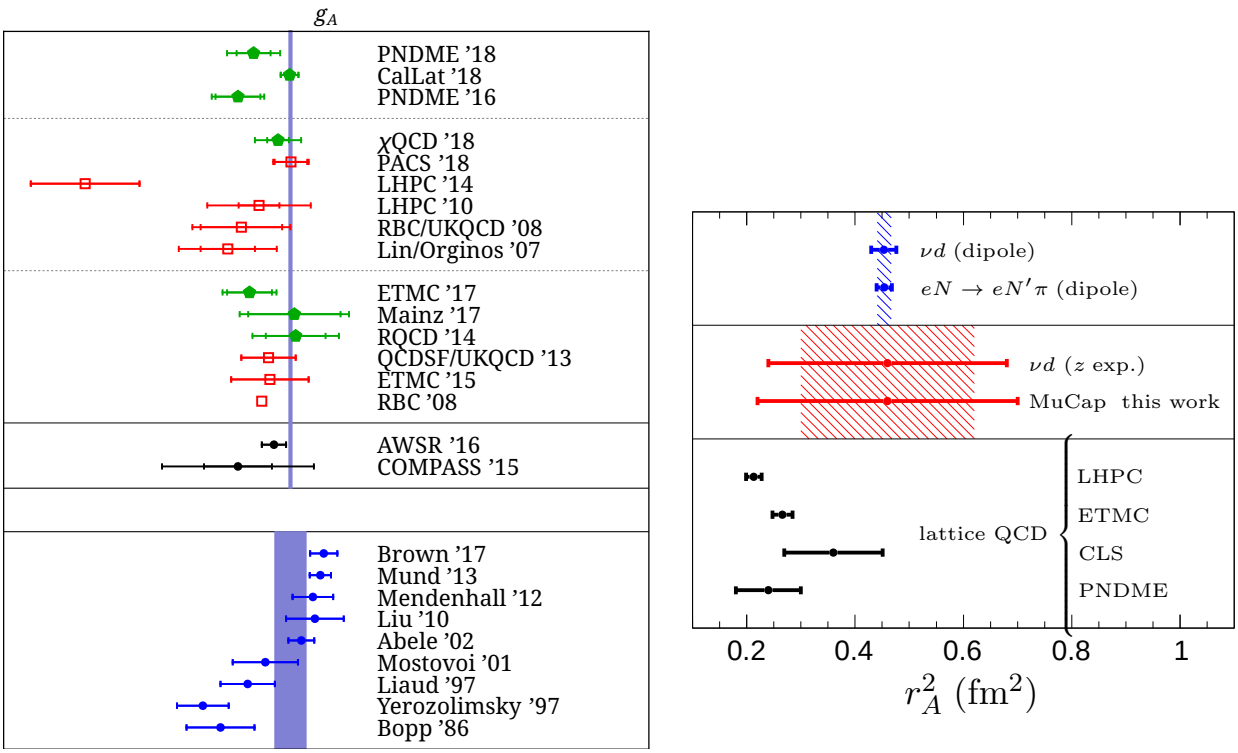

FIG. 5. Status of lattice-QCD calculations of g_A (left) and r_A^2 (right), together with non-lattice determinations. Left: Filled green (unfilled red) lattice-QCD results have (in)complete error budgets. The violet line in the upper panel is the PDG average of the results in the bottom panel, in which the scale is blown up by a factor of 10. Right: As discussed in the text, the error bars on r_A^2 from dipole fits are underestimated and the two small lattice-QCD error bars stem from incomplete error analyses (critiqued below). The references for r_A^2 from top to bottom are as follows: "νd and $eN \to eN'\pi$ (dipole)" [50], "νd (z exp.)" [58], "MuCap this work" [59], LHPC [62] (NB: one lattice spacing and $M_\pi = 317$ MeV), ETMC [63] (NB: no strange sea and a small volume such that $M_\pi L < 3$), CLS [64], PNDME[65]. From Refs. [77] (left) and [59] (right, adapted with permission).

[3] Note that the normalization of the matrix element can be blinded with an multiplicative offset [82], to guard against analyst bias. The results in Fig. 5 (left) have not, however, employed this technique.

dependence of the form factors. It is imperative to use a model-independent parametrization based on general analytic properties. In the complex-q^2 plane, the vector (axial) form factors have a cut starting at $q^2 = t_{\rm cut} \equiv 4M_\pi^2$ ($q^2 = t_{\rm cut} \equiv 9M_\pi^2$) and extending to ∞ on the real axis. The cut lies outside scattering kinematics $q^2 < 0$ but nevertheless prevents a useful series expansion in q^2 around the origin. A rigorous way to proceed is to introduce a conformal mapping that maps the cut to the unit circle [83, 84]:

$$z(t) = \frac{\sqrt{t_{\rm cut} - t} - \sqrt{t_{\rm cut} - t_0}}{\sqrt{t_{\rm cut} - t} + \sqrt{t_{\rm cut} - t_0}}, \tag{2.4}$$

where the parameter t_0 can be chosen to center the q^2 range of interest on $z = 0$; in general, spacelike $q^2 \to -\infty$ maps to $z \to 1$. An expansion of the form

$$F(z) = \sum_k a_k z^k \tag{2.5}$$

thus has an expansion parameter $|z| < 1$. Moreover, unitarity in quantum mechanics ensures that the series is uniformly convergent on this interval. In fact, unitarity leads to bounds on the coefficients a_k that the dipole form, Eq. (2.3), violates [46].

In practice [46, 85–87], the z expansion converges after a few terms. Because on the nonlinear mapping, even an intercept and slope in z give a form factor with a physical shape (i.e., similar to those shown in Fig. 4). As lattice data improve, more and more terms will become resolvable. As in CKM physics [86, 87], lattice-QCD papers can provide the coefficients, their uncertainties, and their correlations; several lattice-QCD calculations of F_A do the same [62–65]. Finally, code for taking such z-expansion input is included in the GENIE event generator [27] module for the axial form factor, and work is underway to extend this to the vector form factor channel.

Although not crucial to neutrino oscillations, the same experiments study weak neutral-current interactions of the Z boson and, possibly, non-Standard bosons [88, 89]. The corresponding Dirac and Pauli form factors can be obtained from the proton and neutron electromagnetic form factors and the strange-quark contribution (accessible in parity-violating elastic electron-scattering experiments [90]) as

$$F_i^{\rm NC} = \left(\tfrac{1}{2} - \sin^2\theta_{\rm W}\right)\left(F_i^{{\rm em},p} - F_i^{{\rm em},n}\right) - \sin^2\theta_{\rm W}\left(F_i^{{\rm em},p} + F_i^{{\rm em},n}\right) - \tfrac{1}{2}F_i^s, \tag{2.6}$$
$$i \in \{1, 2\}.$$

Using the most recent z-expansion fit to nucleon electromagnetic form factors [91] and a new lattice-QCD calculation of strange-quark form factors [92], one can see that the strange-quark contribution increases the neutral-current Pauli form factor, $F_2^{\rm NC}(q^2)$, by about 3.1% and 2.5% at $q^2 = 0$ and $q^2 = -0.1$ GeV^2, respectively. Although the strange-quark contribution is small, the coefficients $(\frac{1}{2} - \sin^2\theta_{\rm W})$ and $\sin^2\theta_{\rm W}$ suppress the two combinations of nucleon electromagnetic form factors in Eq. (2.6), such that the strange-quark sea makes an important contribution to $F_2^{\rm NC}(q^2)$ at low q^2.

Similarly, assuming isospin symmetry and the absence of second-class currents, one can relate the neutral-current axial form factor to the charged-current axial and strange-quark axial form factors [93, 94]:

$$F_A^{\rm NC} = \tfrac{1}{2}(-F_A^{\rm CC} + F_A^s). \tag{2.7}$$

It has been shown [95, 96] that the effect of Pauli blocking becomes very significant in the region $0 < -q^2 \lesssim 0.2$ GeV^2. Therefore, a precise lattice-QCD calculation of $F_A^{\rm NC}(q^2)$ is

required for a precise estimate of the neutral-current (anti)neutrino-nucleon scattering cross section.

Finally, we note that quasielastic neutrino and antineutrino scattering would be sensitive to the presence of the second-class currents, F_S and F_T in Eq. (2.1), characterized by a different G-parity to the standard vector and axial currents of the Standard Model. The search for such currents has long been pursued in the β-decay experiments and in muon-capture experiments, but the measurement of polarization observables in the quasielastic scattering both of nucleons and of hyperons has been shown to be sensitive both to G invariance and to T-invariance [97]. Lattice QCD can contribute to these tests through calculations of induced scalar and tensor currents, including calculations of transition form factors to the rest of the SU(3) baryon octet (Λ and Σ as well as p and n), such as those in Refs. [98, 99].

B. Moments of parton density functions

Lattice QCD can be used to calculate matrix elements of other operators besides the electroweak currents. An important class of operators are those the appear in the operator-product expansion of two currents. Their matrix elements are related to the moments of structure functions in deep-inelastic scattering. For a full discussion, see the USQCD companion white paper "Hadrons and Nuclei" [4]. Here, applications to neutrino physics are discussed.

In 2001, the NuTeV collaboration determined the on-shell weak mixing angle, $\sin^2\theta_W \equiv 1 - m_W^2/m_Z^2$, to be $0.2277 \pm 0.0013_{\rm stat} \pm 0.0009_{\rm syst}$ [100] in deep-inelastic neutrino scattering off iron. This result is 2.7σ discrepant from the current world average of other experiments, 0.22343 ± 0.00007 [49]. This discrepancy, which is known as the "NuTeV anomaly", has no universally accepted explanation, although many possibilities have been raised [101–106].

One suggestion that may account for part of the anomaly is the strange-antistrange parton asymmetry [107, 108], $\langle x \rangle_{s_-} = \int dx\, x\, [s(x) - \bar{s}(x)]$, where $s(x)$ ($\bar{s}(x)$) is the (anti)strange parton distribution function, as a function of parton momentum fraction x. A global analysis of several experimental data sets gives $\langle x \rangle_{s_-} \approx 0.0018$ [109], which is consistent with a 2006 NuTeV analysis of dimuon production [110]. The global analysis does not, however, find a tight constraint: the authors of Ref. [109] present the range $-0.001 < \langle x \rangle_{s_-} < 0.005$ at 90% confidence level.

In view of the uncertain of $\langle x \rangle_{s_-}$ from global fitting, a first-principles lattice-QCD calculation is warranted. There is, however, no local operator which corresponds to $\langle x \rangle_{s_-}$. Instead, one can calculate the third moment from the local operator $\bar{s}\gamma_\mu D_\nu D_\lambda s$ which corresponds to $\langle x^2 \rangle_{s_-} = \int dx\, x^2 (s(x) - \bar{s}(x))$. Assuming $s(x) - \bar{s}(x)$ changes sign only once, $\langle x^2 \rangle_{s_-}$ should give the same sign as that of $\langle x \rangle_{s_-}$. This quantity can also be used to constrain the x-dependent distribution, but since it is expected to be small, calculations will require significant resources.

III. CHALLENGING CALCULATIONS

In this section, calculations that are computationally more difficult than the form factors in Sec. II are discussed. That said, the conceptual formalism underlying these calculations is well established, and pilot calculations provide some idea of how more complete calculations

can be carried out. More complicated final states in the resonance regions (Sec. III A), the shallow inelastic region (Sec. III B), and the deep inelastic region (Sec. III C) are discussed, as are calculations of the axial charge, and related quantities, of small nuclei (Sec. III D).

A. Transition form factors: resonances and multibody final states

Neutrino scattering above the pion-production threshold constitutes the resonance region, where the scattered nucleon is excited into resonances, beginning with the $\Delta(1232)$. To describe the data in this regime thus requires a quantitative knowledge of the $N \to \Delta$ and $N \to N^*$ transitions, mediated through an external current. Because these hadrons are unstable, they can also be viewed as a nucleon with one or more pions, which are the only hadrons composed of the light u/d quarks stable under the strong interaction.

Lattice QCD has a long history of calculations of the transition form factors to the Δ, treating it as stable. Both the vector current [111, 112], and the axial current [113] have been studied with unphysically large quark masses, such that M_Δ at these quark masses lies below the $N\pi$ threshold. These calculations are useful benchmarks for comparisons with non-lattice approaches that neglect the two-body nature of the resonance. Although not as rigorous as the methods discussed below, this "quick and dirty" approach may be timely, for example, providing qualitative input to understand better the MiniBooNE low-energy backgrounds from $\Delta \to N\gamma$ [114].

Because of the finite volume and Euclidean signature, calculations with two-body states in lattice QCD are conceptually and computationally more difficult [115, 116] than the calculations discussed in Sec. II. For example, the Lüscher method [115] relating energy shifts at finite volume to infinite-volume momentum-dependent phase shifts has been used to study the ρ meson [117–121], as well as $I = 2$ $\pi\pi$ phase shifts [122–126] from first principles. The theoretical framework for understanding the transition to multihadron states from Euclidean-space lattice QCD calculations have been further developed over the past several years. Notably, the formalism has been extended both to inelastic scattering [127–131] with several two-body channels, and to three-body scattering [132–137], and there have now been several computational applications of these advances [138–141].

A quantitative understanding of resonance production entails extending the formalism to encompassing transitions mediated through external currents, corresponding here to both vector and axial currents. The needed formalism to two-body final states, and for arbitrary spin, has now been developed [142]. The applications have largely focused on the meson sector. To cite an example bearing some similarity to $W^*n \to \Delta$ in neutrino scattering, the $\gamma^*\pi \to \rho$ transition has been computed in lattice QCD [143, 144], providing the first rigorous calculation of the transition form factor to an unstable hadron, illustrated in Fig. 6 In addition, methods to extract resonance-to-resonance transitions, for example, $\gamma^*\rho \to \rho$, via lattice calculations of two-to-two transition amplitudes, in this case $\gamma^*\pi\pi \to \pi\pi$, have been developed [145, 146]. This opens the possibility for calculations of two-body currents, that is, matrix elements of the form $\langle NN|J^\mu|NN\rangle$ needed for two-nucleon knockout.

Thus, the theoretical underpinnings for understanding resonance production in $\nu N \to \Delta$, N^*, and $N\pi$, are therefore largely in place. Calculations of multihadron states containing baryons are complicated by the extra complexity of the systems relating to the increased number of quarks, by poorer signal-to-noise ratios, and by the larger number of open channels. Even so, the first *ab initio* determination of $\Delta(1232)$ resonance parameters appeared in 2017 [147], albeit for a simulation with quark masses corresponding to a pion mass of

280 MeV, yielding a Δ-N-π coupling in agreement with phenomenological determinations. As the invariant mass of the system increases within the resonance regime and the pion mass is decreased to its physical value, however, inelastic processes and three- and higher-body final states become relevant. Further theoretical work is needed to encompass transitions to three or more particles, and further development of efficient algorithms is needed to evaluate the larger number of Wick contractions that increasingly dominate the computational cost of the calculation. The interplay between theoretical methods and practical algorithms is, of course, ideally researched on high-capacity computing facilities.

B. Hadron tensor for shallow and deep inelastic scattering

At higher energies, more and more pions are produced and a full theoretical description of any given final state becomes impractical. One can, however, study the sum over all final states via the optical theorem and consider forward matrix elements of the product of two currents. Whereas nuclear many-body theory decomposes the low-multiplicity cases into products of nuclear wavefunctions and nucleon (and $N\pi$, ...) form factors, here one can decompose the nuclear hadron tensor, $\langle A|J_\mu^\dagger J_\nu|A\rangle$, into a spectral function [148] and the nucleon hadron tensor, $\langle N|J_\mu^\dagger J_\nu|N\rangle$. A recent development in lattice QCD is to calculate this quantity from a four-point correlation function. This approach is especially appealing in the region, sometimes called shallow inelastic, between the resonances and deep-inelastic scattering, where no other theoretical tool holds much promise [16].

The Euclidean hadronic tensor [149–156] can be decomposed in terms of structure functions that are related to their Minkowski counterparts through a Laplace transform. Thus, to obtain the desired structure functions, an inverse Laplace transform is needed, an ill-posed

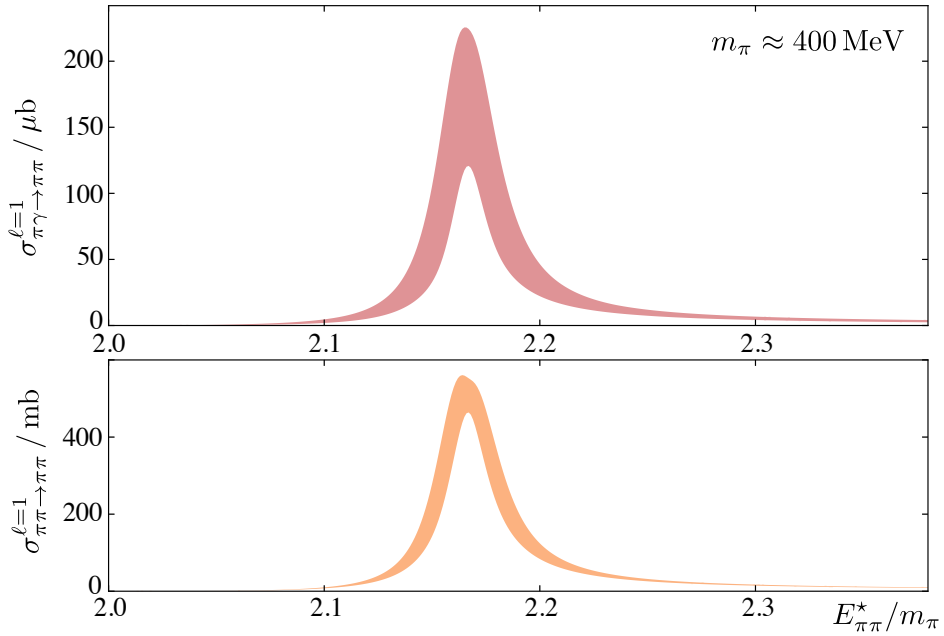

FIG. 6. The upper and lower panels show the $\gamma^*\pi^+ \to \pi^+\pi^0$ and $l = 1$ elastic $\pi\pi$ scattering cross sections, respectively, as a function of $\pi\pi$ energy, with the ρ resonance clearly visible [142].

problem that arises in many fields. Three approaches to this problem are the maximum entropy method (MEM) [151], the MEM with a prior to stabilize the fit for Bayesian reconstruction (MEM-BR) [154], and the Backus-Gilbert method [156]. These three numerical approaches have been studied recently [157]. The Backus-Gilbert method yields a single broad peak in the energy spectrum from lattice data with 20 points in Euclidean time. With both the MEM and MEM-BR, the elastic peak and the resonance peak are resolved, with the MEM-BR producing sharper peaks and a more stable reconstruction. Given the test lattice spacing of 0.12 fm, there is no excitation spectrum above 2 GeV and, thus, no strength in the spectral weight above the resonance region. For a finer lattice with spacing 0.04 fm, the spectral weight up to 5 GeV is accessible. Even though it may still not be sufficient to resolve the individual resonances, the fact it can cover both the resonance and the shallow inelastic scattering regions makes the lattice hadronic tensor calculation a promising theoretical tool to address the total cross section of the neutrino-nucleus scattering over a wide range of energy transfers up to 5 GeV.

The hadron tensor can also be computed for deep-inelastic scattering. In this case, the calculation needs to be able to access the kinematic region where $Q^2 > 4$ GeV^2 and energy transfer $\nu > 5$ GeV where the higher-twist contributions are suppressed. The Euclidean correlation function can also be analyzed with the OPE, along the lines of the suggestion for calculating the shape function of the inclusive B-meson semileptonic decay rate [152]. In addition, using a fictitious heavy-quark propagator between the currents to calculate moments has been proposed [153]. A related approach is also discussed in Ref. [155]. Unlike the approaches discussed in the next subsection, the hadron-tensor approach to deep-inelastic scattering does not need to match to the infinite-momentum frame.

C. Parton densities for neutrino deep-inelastic scattering

The parton distribution functions (PDFs) will be important inputs in the upcoming precision neutrino-physics experiments, particularly at large Bjorken x and at the highest energies of the DUNE beam, $\sim$ 4–5 GeV. For these kinematics, current global-fit PDFs either suffer greatly from the theoretical uncertainty in their nuclear treatment or rely mainly on extrapolation from intermediate x.

Direct calculation of the Bjorken x dependence of hadron structure in lattice QCD has only recently become possible thanks to the development of the large-momentum effective theory (LaMET) [158], which introduces a large momentum P to connect Euclidean lattice QCD to the desired Minkowski distributions.[4] This framework has allowed the first direct lattice-QCD computations of the x dependence of parton distributions [162]. Further developments spurred on by these developments include that of pseudo-PDFs [163], and that of matrix elements of gauge-invariant current-current correlators [164]. In these new approaches, valence- and sea-quark structure can be disentangled, which leads to the possibility of using lattice-QCD calculations to directly compare with experiments on large-x structure in SoLID at Jefferson Lab, with sea structure in Drell-Yan experiments at Fermilab or with data from a future electron-ion collider. In addition to the hadron-tensor method described in the previous subsection, these new approaches and numerical investigations thereof are described in detail in the companion whitepaper "Hadrons and Nuclei" [4].

[4] See Refs. [159–161] for critical discussions of this approach.

The lattice-QCD effort so far has focused on isovector combinations of PDFs, that is, the difference between the up and down distributions. A recent joint lattice-QCD and global-fitting community report [38], an effort led by USQCD members, demonstrated that a calculation of the isovector proton PDF at the 12% level for $x \in [0.7, 0.9]$ can impact our knowledge of the PDF at x near 1 by more than 20%. This kinematic region is relevant for neutrino experiments, and such precision should be feasible in the near term. In addition, as crosscheck of nuclear theory in this region, exploratory calculations of nuclear PDFs will become available; see Sec. III D. Such precision is already relevant to neutrino-nucleon scattering at 4–5 GeV. Further, it allows a crosscheck of the nuclear-theory treatment and of the systematic uncertainties of nuclear PDFs.

Neutrino DIS can be important for determining the strange quark and antiquark parton distributions. Currently, no calculation of the Bjorken-x dependence of the strange PDF has been done with lattice QCD, due to numerical limitations, but there are USQCD proposals to investigate $s(x) - \bar{s}(x)$. On the other hand, the nucleon sea flavor asymmetry $\bar{u}(x) - \bar{d}(x)$ has been studied [165]. Unfortunately, the uncertainties in the quasi-PDF approach are currently much larger than those from experimental/phenomenological extraction.

Going to larger nucleon boost momenta P with high statistics is key to reducing several systematic uncertainties in these quasi-PDF and pseudo-PDF approaches [4], especially for the antiquark distribution and small Bjorken x. However, this poses several computational challenges. First, large momentum translates into large $(aP)^n$, and therefore, ensembles with increasingly smaller lattice spacings a are needed. Given the need to keep the spatial size of the box sufficiently large to avoid significant finite-volume effects, which may be enhanced for some nonlocal matrix elements [166], this increases the computational cost. Second, as the momentum becomes larger, the signal-to-noise ratio degrades, even when using methods such as "momentum smearing"[167], designed to enhance the contribution of the lowest-lying state in correlation functions at nonzero three-momentum, thereby increasing the number of measurements that need to be made. Last, the excited-state contributions themselves become more significant at higher momenta both through the greater number of contributing states arising from the reduced symmetries at nonzero momentum, and through the relative compression of the energy spectrum. This requires either calculations at many source-sink separations, or the use of the variational method with an expanded basis of operators. Thus calculations of the precision that the neutrino program demands requires a significant commitment of computational resources.

D. Axial currents in light nuclei

An important challenge for lattice QCD is to extend the calculations of the axial properties of the nucleon to the more complex systems of nuclei. Just as for the nucleon, knowing nuclear matrix elements of axial currents and of quantities relevant in deep-inelastic scattering on nuclei are high priorities in the lattice-QCD community. Over the last decade, first studies of a range of nuclear properties have been performed, and calculations of the requisite axial structure of light nuclei are eminently feasible in a five-year timeframe.

Nuclear effects in neutrino-nucleus scattering are important, extremely nontrivial, and not simply related to those in electron-nucleus scattering. For example, Gamow-Teller transitions in nuclei [168–170], which flip spin and isospin of the nucleus, are poorly described in most simple nuclear models, with deviations of as much as 25% from naive expectations based on simply scaling from the single-particle $n \to pe\bar{\nu}$ transition. Once sophisticated nu-

clear wave functions and many-body axial currents [171, 172] are used, however, agreement with the data is reached [173]. At higher energies, state-of-the-art Green-function Monte-Carlo (an exact many-body method) calculations [174, 175] show that neutrino response functions describing scattering on nuclei such as ^{12}C have effects from two-body currents at the 20% level, particularly in the transverse response.

In the last few years, USQCD collaboration members have performed lattice-QCD calculations of $A = 2, 3$ axial transitions in the forward limit using unphysically heavy quark masses corresponding to $M_\pi \sim 800$ MeV [176–178]. This work, in which the Gamow-Teller contribution to tritium β-decay and the rate of the $pp \to de\bar{\nu}$ fusion process were extracted, demonstrates that the calculations relevant to constrain neutrino interactions with light nuclei can be performed. While nuclear effects in the axial matrix elements of two- and three-body systems are found to be at the few percent level, the lattice-QCD calculations were able to resolve the relevant effects by isolating the intrinsically two-body contributions. Pursuing these calculations at the physical quark masses and controlling all sources of systematic uncertainties in them will require exascale computing resources. Beyond these forward limit calculations, extensions of this approach to enable calculations of the form factors of light nuclei from nonforward transition matrix elements are underway. Calculations involving multiparticle final states are also necessary but challenging: a theoretical understanding of the simplest inelastic channels is presented in Ref. [145]. For high-energy neutrino-nucleus scattering in the deep-inelastic regime, lattice-QCD calculations of the moments of the relevant parton distributions in nuclei will be useful in constraining nuclear effects in a very different kinematic regime.

While these calculations do not directly address the particular nuclear targets for DUNE and other neutrino-scattering experiments, they are useful in constraining the low-energy constants and meson-exchange currents that enter nuclear-chiral-EFT axial currents [171, 172]. Such matchings are already underway for spectroscopy [179–181] and electromagnetic interactions [182] at unphysical values of the quark masses, and the machinery necessary to undertake this at the physical quark masses is being developed. As well as studies of currents, lattice-QCD calculations of nuclei and other systems such as three and four neutron systems will provide input into the three-body forces in nuclear EFTs, particularly those aspects of these forces that are challenging to access experimentally.

IV. EXTREMELY CHALLENGING CALCULATIONS

Looking further into the future, we can foresee the need for calculations that go far enough beyond the current state of the art that it is hard to know when or whether they will be possible.

A. Electromagnetic and isospin-breaking effects

Going beyond the leading order, calculations of nucleon matrix elements must incorporated the neglected contributions from both QED and from strong isospin breaking (SIB). There are two possible approaches for completing these tasks, which can be generally classified as being perturbative and nonperturbative. Perturbative calculations make use of existing isospin-symmetric and QCD-only lattice ensembles to compute the desired matrix elements. The QED effects are computed with explicit vector current insertions and some

scheme for the virtual photon lines. Similarly, the SIB effects are included via scalar current insertions that allow for expansion in quark mass about the isospin-symmetric point. For nucleon matrix elements, perturbative calculations require five-point correlation functions as well as disconnected diagrams and and pose a significant challenge to pursue.

Nonperturbative calculations make use of gauge ensembles that include explicit sea effects for QED and SIB. These are SU(3) × U(1) gauge field ensembles with the up and down quark masses tuned to their physical values. Rather than being restricted to a perturbative expansion of photon fields, these calculations include combined gluon, photon, and quark loops to all orders. While these calculations are likely to be cheaper than the perturbative calculations mentioned above, they also have technical difficulties that must be overcome. The most challenging of these difficulties is likely to come from finite size effects. Since photons mediate a long range force, calculations including QED will be sensitive to the size of the lattice. Many computations on lattice ensembles with different volumes will be necessary to quantify and remove this systematic effect.

B. Axial currents in heavier nuclei

A holy grail for neutrino-nucleus scattering is controlled QCD calculations of the axial form factors, resonance transition form factors, and nuclear PDFs for ^{40}Ar, the target nucleus in DUNE and several other experiments. As yet, exponentially hard challenges must be overcome in order for meaningful lattice-QCD calculations of such heavy nuclei. Both the factorial growth complexity of many-body contractions and the exponentially degradation of the signal-to-noise ratio are currently impede to progress on this front. Since lattice-QCD studies of nuclei are relatively new, it is not unlikely that new algorithms will definitively alter this picture (algorithms involving machine learning and quantum computation [183] may dramatically improve the situation),[5] but at present it is realistic to assume that direct lattice-QCD calculations of argon will not occur in a timeframe relevant for the coming long-baseline experiments.

Perhaps more realistically, significant tests of nuclear EFT frameworks beyond the few-body sector would be enabled by lattice-QCD calculations of the spectrum and axial structure of an intermediate nucleus such as ^{12}C. Aspects of coherent scattering off nuclei will also be addressed by such calculations. While still challenging, a number of groups are investigating ways to perform the relevant contractions and studying improved ways to extract signals from noisy multi-baryon data through optimization methods [184] or improved estimators [43, 185–188]. For carbon targets, experimental scattering data exists and comparison of lattice-QCD calculations with this will help understand the systematics of the A dependence of nuclear EFT approaches and assess the reliability of the extrapolations to argon.

For light nuclei, adapting the techniques discussed above to address the Bjorken-x dependence on nuclear PDFs will become possible as computing resources increase. While challenging, and still in the development stage even for the nucleon, these PDF methods will help constrain the flavor and spin dependence of nuclear PDFs that are important for high-energy νA scattering.

[5] For discussion of these novel approaches, see the companion whitepaper "Status and Future Perspectives for Lattice Gauge Theory Calculations to the Exascale and Beyond" [5].

V. COMPUTING NEEDS

As we have seen in Secs. III and IV, many topics pertaining to lattice QCD for neutrino physics are still exploratory. In those cases, computing estimates are impossible because progress depends on innovation and flexible computing, rather than an industrial resource. It is feasible and reasonable, however, to estimate the computing needs of the calculations discussed in Sec. II. We do so here, focusing on the example of nucleon form factors.

The methodology for the calculation of the axial and the electromagnetic form factors is well established, and data with control over statistical errors have been generated by several collaborations worldwide. Table I list several of these efforts. Unfortunately, only a few include several ensembles with strange sea quarks [65, 68, 71]. Even those calculations should be pushed to smaller lattice spacing and (in one case) smaller up-down quark mass. Furthermore, most calculations obtain mean-squared charge radii (r_A, r_E, and r_M) that are smaller than phenomenological extractions, by about 30%. To diagnose where the difference lies, it is crucial to improve control over systematic uncertainties in lattice-QCD calculations to obtain a definitive result from QCD.

Here we base the cost estimates for achieving a 10–15% result on two ongoing efforts within USQCD. A convenient starting point is the work of PNDME collaboration that has presented extensive results for the axial form factors [65] using the Wilson-clover formulation for the valence quarks on ensembles with 2+1+1 sea quarks with the staggered formulation. One way to avoid this "mixed action" approach is to use staggered valence quarks [82]. Based on current running on institutional clusters at BNL and Fermilab, we estimate 9M GPU-hours[6] to carry out a calculation on eleven ensembles, five at physical sea-quark mass, and six with $m_l = \frac{1}{2}(m_u + m_d) = 0.2m_s$, with lattice spacing as small as 0.03 fm.

TABLE I. Sample of calculations of nucleon form factors going on worldwide. In the first column, "2", "2+1", and "2+1+1" all denote two equal-mass quarks for up and down; the latter two include strange and charm, respectively. The last column indicates work in which USQCD members participate.

Sea quarks	Valence quarks	$N_{\rm ens}$	a (fm)	M_π (MeV)	Collaboration	Ref.	USQCD
2 Wilson-clover	same as sea	11	0.06–0.08	150–490	RQCD	[60]	
2 TM clover	same as sea	1	0.09	130	ETM	[63]	
2 Wilson-clover	same as sea	11	0.05–0.08	190–470	Mainz (CLS)	[64]	
2+1 overlap	same as sea	4	0.11	290–540	JLQCD	[67]	
2+1 domain wall [45]	overlap	3	0.08–0.15	170–340	χQCD	[70]	✓
2+1 Wilson-clover	same as sea	1	0.085	146, 135	PACS	[73]	
2+1 Wilson-clover	same as sea	11	0.05–0.09	200–350	Mainz (CLS)	[71]	
2+1+1 HISQ [40]	Wilson-clover	8	0.06–0.12	135–210	PNDME	[65]	✓
2+1+1 HISQ [40]	domain wall	16	0.09–0.15	130–400	CalLat	[68]	✓
2+1+1 TM clover	same as sea	3	0.09–0.15	140	ETM	[74]	✓
2+1+1 HISQ	same as sea	3	0.09–0.15	135	Fermilab/MILC	[82]	✓

[6] For QCD codes, these 9M GPU hours correspond to 300M conventional (e.g., Intel Skylake) CPU core-hours.

Similarly, a significant subset of USQCD plans on generating a suite of ensembles with Wilson-clover sea quarks. To generate eight such ensembles, with light sea-quark masses corresponding to pion masses of 170 MeV and 270 MeV (four ensembles each), with lattice spacing as small as 0.05 fm. The estimate to finish generating these ensembles is 8M GPU-hours (assuming the GPUs on Summit at ORNL). This chunk of computing will be shared with many other projects, particularly those described in the companion white paper "Hadrons and Nuclei" [4]. The computation of the needed nucleon correlation functions is estimated to require 15M GPU-hours.

These estimates set the scale for a modern calculation of the simplest quantity needed for neutrino physics. At the same time, comparably demanding work with small nuclei, but not yet physical pion mass, will be needed. Such work is necessary to understand the technical issues facing more realistic calculations and to find better methods and algorithms. Even assuming gains from innovation, it is hard to imagine that nuclear form factors will end up below 10M GPU-hours. The same line of reasoning can be applied to other calculations discussed in Sec. III.

ACKNOWLEDGMENTS

We would like to thank Raúl Briceño, Maxwell Hansen, Richard Hill, Ciaran Hughes, William Marciano, Saori Pastore, Noemi Rocco, and Michael Wagman for useful input. This material is based upon work supported by the U.S. Department of Energy, Office of Science, Office of Nuclear Physics under contract No. DE-AC05-06OR23177. Fermilab is operated by Fermi Research Alliance, LLC, under Contract No. DE-AC02-07CH11359 with the United States Department of Energy, Office of Science, Office of High Energy Physics.

[1] Alexei Bazavov, Frithjof Karsch, Swagato Mukherjee, and Peter Petreczky (USQCD), "Hot-dense lattice QCD," (2019).

[2] Richard Brower, Anna Hasenfratz, Ethan T. Neil, *et al.* (USQCD), "Lattice gauge theory for physics beyond the Standard Model," (2019).

[3] Vincenzo Cirigliano, Zohreh Davoudi, *et al.* (USQCD), "The role of lattice QCD in searches for violations of fundamental symmetries and signals for new physics," (2019).

[4] William Detmold, Robert G. Edwards, *et al.* (USQCD), "Hadrons and nuclei," (2019).

[5] Bálint Joó, Chulwoo Jung, *et al.* (USQCD), "Status and future perspectives for lattice gauge theory calculations to the exascale and beyond," (2019).

[6] Christoph Lehner, Stefan Meinel, *et al.* (USQCD), "Opportunities for lattice QCD in quark and lepton flavor physics," (2019).

[7] Y. Fukuda *et al.* (Super-Kamiokande), "Evidence for oscillation of atmospheric neutrinos," Phys. Rev. Lett. **81**, 1562–1567 (1998), arXiv:hep-ex/9807003 [hep-ex].

[8] Q. R. Ahmad *et al.* (SNO), "Measurement of the rate of $\nu_e + d \to p + p + e^-$ interactions produced by ^{8}B solar neutrinos at the Sudbury Neutrino Observatory," Phys. Rev. Lett. **87**, 071301 (2001), arXiv:nucl-ex/0106015 [nucl-ex].

[9] R. Acciarri *et al.* (DUNE), "Long-Baseline Neutrino Facility (LBNF) and Deep Underground Neutrino Experiment (DUNE)," (2015), arXiv:1512.06148 [physics.ins-det].

[10] K. Abe *et al.* (Hyper-Kamiokande), "Hyper-Kamiokande design report," (2018), arXiv:1805.04163 [physics.ins-det].

[11] Ettore Majorana, "Teoria simmetrica dellelettrone e del positrone," Nuovo Cim. **14**, 171–184 (1937).

[12] Peter Minkowski, "$\mu \to e\gamma$ at a rate of one out of 10^9 muon decays?" Phys. Lett. **67B**, 421–428 (1977); Tsutomu Yanagida, "Horizontal symmetry and masses of neutrinos," Prog. Theor. Phys. **64**, 1103 (1980); Murray Gell-Mann, Pierre Ramond, and Richard Slansky, "Complex spinors and unified theories," in *Supergravity*, edited by P. van Nieuwenhuizen (North-Holland, Amsterdam, 1979) pp. 315–321, arXiv:1306.4669 [hep-th].

[13] B. Pontecorvo, "Mesonium and antimesonium," Sov. Phys. JETP **6**, 429 (1957), [Zh. Eksp. Teor. Fiz. **33**, 549 (1957)]; "Neutrino experiments and the problem of conservation of leptonic charge," **26**, 984–988 (1968), [Zh. Eksp. Teor. Fiz. **53**, 1717 (1967)]; Ziro Maki, Masami Nakagawa, and Shoichi Sakata, "Remarks on the unified model of elementary particles," Prog. Theor. Phys. **28**, 870–880 (1962).

[14] Nicola Cabibbo, "Unitary symmetry and leptonic decays," Phys. Rev. Lett. **10**, 531–533 (1963); Makoto Kobayashi and Toshihide Maskawa, "CP violation in the renormalizable theory of weak interaction," Prog. Theor. Phys. **49**, 652–657 (1973).

[15] Laura Fields, private communication (2018).

[16] L. Alvarez-Ruso *et al.* (NuSTEC), "NuSTEC white paper: Status and challenges of neutrino-nucleus scattering," Prog. Part. Nucl. Phys. **100**, 1–68 (2018), arXiv:1706.03621 [hep-ph].

[17] Omar Benhar and Alessandro Lovato, "Towards a unified description of the electroweak nuclear response," Int. J. Mod. Phys. **E24**, 1530006 (2015), arXiv:1506.05225 [nucl-th].

[18] J. Carlson, S. Gandolfi, F. Pederiva, Steven C. Pieper, R. Schiavilla, K. E. Schmidt, and R. B. Wiringa, "Quantum Monte Carlo methods for nuclear physics," Rev. Mod. Phys. **87**, 1067 (2015), and references within, arXiv:1412.3081 [nucl-th].

[19] Evgeny Epelbaum, Hans-Werner Hammer, and Ulf-G. Meissner, "Modern theory of nuclear forces," Rev. Mod. Phys. **81**, 1773–1825 (2009), arXiv:0811.1338 [nucl-th].

[20] R. Machleidt and D. R. Entem, "Chiral effective field theory and nuclear forces," Phys. Rept. **503**, 1–75 (2011), arXiv:1105.2919 [nucl-th].

[21] Steven Weinberg, "Nuclear forces from chiral Lagrangians," Phys. Lett. **B251**, 288–292 (1990).

[22] U. van Kolck, "Few nucleon forces from chiral Lagrangians," Phys. Rev. **C49**, 2932–2941 (1994).

[23] David B. Kaplan, Martin J. Savage, and Mark B. Wise, "A new expansion for nucleon-nucleon interactions," Phys. Lett. **B424**, 390–396 (1998), arXiv:nucl-th/9801034 [nucl-th].

[24] Ulf-G Meiner, "The long and winding road from chiral effective Lagrangians to nuclear structure," Phys. Scripta **91**, 033005 (2016), arXiv:1510.03230 [nucl-th].

[25] Cezary Juszczak, Jaroslaw A. Nowak, and Jan T. Sobczyk, "Simulations from a new neutrino event generator," Nucl. Phys. Proc. Suppl. **159**, 211–216 (2006), arXiv:hep-ph/0512365 [hep-ph]; Jakub muda, Krzysztof M. Graczyk, Cezary Juszczak, and Jan T. Sobczyk, "NuWro Monte Carlo generator of neutrino interactions—first electron scattering results," Acta Phys. Polon. **B46**, 2329 (2015), arXiv:1510.03268 [hep-ph].

[26] Yoshinari Hayato, "A neutrino interaction simulation program library NEUT," Acta Phys. Polon. **B40**, 2477–2489 (2009).

[27] C. Andreopoulos *et al.*, "The GENIE neutrino Monte Carlo generator," Nucl. Instrum. Meth. **A614**, 87–104 (2010), arXiv:0905.2517 [hep-ph]; M. Alam *et al.*, "GENIE production release

2.10.0," (2015), arXiv:1512.06882 [hep-ph].
[28] K. Gallmeister, U. Mosel, and J. Weil, "Neutrino-induced reactions on nuclei," Phys. Rev. **C94**, 035502 (2016), arXiv:1605.09391 [nucl-th].
[29] D. Casper, "The Nuance neutrino physics simulation, and the future," Nucl. Phys. Proc. Suppl. **112**, 161–170 (2002), arXiv:hep-ph/0208030 [hep-ph].
[30] Jorge Morfín, "Past and future of $\nu/\bar{\nu}$ deuterium/hydrogen experiments," talk at INT Seattle (2018).
[31] D. Androi *et al.* (Qweak), "Precision measurement of the weak charge of the proton," Nature **557**, 207–211 (2018).
[32] Daniel Z. Freedman, "Coherent neutrino nucleus scattering as a probe of the weak neutral current," Phys. Rev. **D9**, 1389–1392 (1974).
[33] S. J. Brice *et al.*, "A method for measuring coherent elastic neutrino-nucleus scattering at a far off-axis high-energy neutrino beam target," Phys. Rev. **D89**, 072004 (2014), arXiv:1311.5958 [physics.ins-det].
[34] D. Akimov *et al.* (COHERENT), "Observation of coherent elastic neutrino-nucleus scattering," Science **357**, 1123–1126 (2017), arXiv:1708.01294 [nucl-ex].
[35] J. A. Formaggio and G. P. Zeller, "From eV to EeV: Neutrino cross sections across energy scales," Rev. Mod. Phys. **84**, 1307–1341 (2012), arXiv:1305.7513 [hep-ex].
[36] J. Carlson and R. Schiavilla, "Structure and dynamics of few nucleon systems," Rev. Mod. Phys. **70**, 743–842 (1998).
[37] Sonia Bacca and Saori Pastore, "Electromagnetic reactions on light nuclei," J. Phys. **G41**, 123002 (2014), arXiv:1407.3490 [nucl-th].
[38] Huey-Wen Lin *et al.*, "Parton distributions and lattice QCD calculations: A community white paper," Prog. Part. Nucl. Phys. **100**, 107–160 (2018), arXiv:1711.07916 [hep-ph].
[39] S. Dürr *et al.* (Budapest-Marseille-Wuppertal), "Lattice QCD at the physical point: Simulation and analysis details," JHEP **08**, 148 (2011), arXiv:1011.2711 [hep-lat].
[40] A. Bazavov *et al.* (MILC), "Lattice QCD ensembles with four flavors of highly improved staggered quarks," Phys. Rev. **D87**, 054505 (2013), arXiv:1212.4768 [hep-lat]; A. Bazavov *et al.* (Fermilab Lattice, MILC), "B- and D-meson leptonic decay constants from four-flavor lattice QCD," Phys. Rev. **D98**, 074512 (2018), arXiv:1712.09262 [hep-lat].
[41] G. Parisi, "The strategy for computing the hadronic mass spectrum," Phys. Rept. **103**, 203–211 (1984).
[42] G. Peter Lepage, "The analysis of algorithms for lattice field theory," in *From Actions to Answers*, edited by T. DeGrand and W. D. Toussaint (World Scientific, Singapore, 1989) pp. 97–120.
[43] Michael L. Wagman, *Statistical Angles on the Lattice QCD Signal-to-Noise Problem*, Ph.D. thesis, University of Washington (2017), arXiv:1711.00062 [hep-lat].
[44] Benjamin J. Owen, Jack Dragos, Waseem Kamleh, Derek B. Leinweber, M. Selim Mahbub, Benjamin J. Menadue, and James M. Zanotti, "Variational approach to the calculation of g_A," Phys. Lett. **B723**, 217–223 (2013), arXiv:1212.4668 [hep-lat].
[45] T. Blum *et al.* (RBC, UKQCD), "Domain wall QCD with physical quark masses," Phys. Rev. **D93**, 074505 (2016), arXiv:1411.7017 [hep-lat].
[46] Bhubanjyoti Bhattacharya, Richard J. Hill, and Gil Paz, "Model independent determination of the axial mass parameter in quasielastic neutrino-nucleon scattering," Phys. Rev. **D84**, 073006 (2011), arXiv:1108.0423 [hep-ph].

[47] Steven Weinberg, "Charge symmetry of weak interactions," Phys. Rev. **112**, 1375–1379 (1958).

[48] C. H. Llewellyn Smith, "Neutrino reactions at accelerator energies," Phys. Rept. **3**, 261–379 (1972).

[49] M. Tanabashi *et al.* (Particle Data Group), "Review of particle physics," Phys. Rev. **D98**, 030001 (2018).

[50] A. Bodek, S. Avvakumov, R. Bradford, and Howard S. Budd, "Vector and axial nucleon form factors: A duality constrained parameterization," Eur. Phys. J. **C53**, 349–354 (2008), arXiv:0708.1946 [hep-ex].

[51] A. Liesenfeld *et al.* (A1), "A measurement of the axial form-factor of the nucleon by the $p(e, e'\pi^+)n$ reaction at $W = 1125$ MeV," Phys. Lett. **B468**, 20 (1999), arXiv:nucl-ex/9911003 [nucl-ex].

[52] Veronique Bernard, Norbert Kaiser, and Ulf G. Meissner, "Measuring the axial radius of the nucleon in pion electroproduction," Phys. Rev. Lett. **69**, 1877–1879 (1992).

[53] R. Gran *et al.* (K2K), "Measurement of the quasielastic axial vector mass in neutrino-oxygen interactions," Phys. Rev. **D74**, 052002 (2006), arXiv:hep-ex/0603034 [hep-ex].

[54] M. Dorman (MINOS), "Preliminary results for CCQE scattering with the MINOS near detector," AIP Conf. Proc. **1189**, 133–138 (2009).

[55] A. A. Aguilar-Arevalo *et al.* (MiniBooNE), "First measurement of the muon neutrino charged current quasielastic double differential cross section," Phys. Rev. **D81**, 092005 (2010), arXiv:1002.2680 [hep-ex].

[56] V. Lyubushkin *et al.* (NOMAD), "A study of quasielastic muon neutrino and antineutrino scattering in the NOMAD experiment," Eur. Phys. J. **C63**, 355–381 (2009), arXiv:0812.4543 [hep-ex].

[57] L. Fields *et al.* (MINERvA), "Measurement of muon antineutrino quasielastic scattering on a hydrocarbon target at $e_\nu \sim 3.5$ GeV," Phys. Rev. Lett. **111**, 022501 (2013), arXiv:1305.2234 [hep-ex]; G. A. Fiorentini *et al.* (MINERvA), "Measurement of muon neutrino quasielastic scattering on a hydrocarbon target at $e_\nu \sim 3.5$ GeV," Phys. Rev. Lett. **111**, 022502 (2013), arXiv:1305.2243 [hep-ex].

[58] Aaron S. Meyer, Minerba Betancourt, Richard Gran, and Richard J. Hill, "Deuterium target data for precision neutrino-nucleus cross sections," Phys. Rev. **D93**, 113015 (2016), arXiv:1603.03048 [hep-ph].

[59] Richard J. Hill, Peter Kammel, William J. Marciano, and Alberto Sirlin, "Nucleon axial radius and muonic hydrogen: A new analysis and review," Rept. Prog. Phys. **81**, 096301 (2018), arXiv:1708.08462 [hep-ph].

[60] Gunnar S. Bali, Sara Collins, Benjamin Glßle, Meinulf Gckeler, Johannes Najjar, Rudolf H. Rdl, Andreas Schfer, Rainer W. Schiel, Wolfgang Sldner, and Andr Sternbeck, "Nucleon isovector couplings from $N_f = 2$ lattice QCD," Phys. Rev. **D91**, 054501 (2015), arXiv:1412.7336 [hep-lat].

[61] Tanmoy Bhattacharya, Vincenzo Cirigliano, Saul Cohen, Rajan Gupta, Huey-Wen Lin, and Boram Yoon, "Axial, scalar and tensor charges of the nucleon from 2+1+1-flavor lattice QCD," Phys. Rev. **D94**, 054508 (2016), arXiv:1606.07049 [hep-lat].

[62] Jeremy Green, Nesreen Hasan, Stefan Meinel, Michael Engelhardt, Stefan Krieg, Jesse Laeuchli, John Negele, Kostas Orginos, Andrew Pochinsky, and Sergey Syritsyn, "Up, down, and strange nucleon axial form factors from lattice QCD," Phys. Rev. **D95**, 114502 (2017), arXiv:1703.06703 [hep-lat].

[63] Constantia Alexandrou, Martha Constantinou, Kyriakos Hadjiyiannakou, Karl Jansen, Christos Kallidonis, Giannis Koutsou, and Alejandro Vaquero Aviles-Casco, "Nucleon axial form factors using $N_f = 2$ twisted mass fermions with a physical value of the pion mass," Phys. Rev. **D96**, 054507 (2017), arXiv:1705.03399 [hep-lat].

[64] Stefano Capitani, Michele Della Morte, Dalibor Djukanovic, Georg M. von Hippel, Jiayu Hua, Benjamin Jger, Parikshit M. Junnarkar, Harvey B. Meyer, Thomas D. Rae, and Hartmut Wittig, "Isovector axial form factors of the nucleon in two-flavor lattice QCD," Int. J. Mod. Phys. **A34**, 1950009 (2019), arXiv:1705.06186 [hep-lat].

[65] Rajan Gupta, Yong-Chull Jang, Huey-Wen Lin, Boram Yoon, and Tanmoy Bhattacharya (PNDME), "Axial vector form factors of the nucleon from lattice QCD," Phys. Rev. **D96**, 114503 (2017), arXiv:1705.06834 [hep-lat].

[66] Yong-Chull Jang, Tanmoy Bhattacharya, Rajan Gupta, Huey-Wen Lin, and Boram Yoon, "Nucleon axial and electromagnetic form factors," EPJ Web Conf. **175**, 06033 (2018), arXiv:1801.01635 [hep-lat].

[67] Nodoka Yamanaka, Shoji Hashimoto, Takashi Kaneko, and Hiroshi Ohki (JLQCD), "Nucleon charges with dynamical overlap fermions," Phys. Rev. **D98**, 054516 (2018), arXiv:1805.10507 [hep-lat].

[68] C. C. Chang *et al.* (CalLat), "A per-cent-level determination of the nucleon axial coupling from quantum chromodynamics," Nature **558**, 91–94 (2018), arXiv:1805.12130 [hep-lat].

[69] Ken-Ichi Ishikawa, Yoshinobu Kuramashi, Shoichi Sasaki, Natsuki Tsukamoto, Akira Ukawa, and Takeshi Yamazaki (PACS), "Nucleon form factors on a large volume lattice near the physical point in 2+1 flavor QCD," Phys. Rev. **D98**, 074510 (2018), arXiv:1807.03974 [hep-lat].

[70] Jian Liang, Yi-Bo Yang, Terrence Draper, Ming Gong, and Keh-Fei Liu (χQCD), "Quark spins and anomalous Ward identity," Phys. Rev. **D98**, 074505 (2018), arXiv:1806.08366 [hep-ph].

[71] Konstantin Ottnad, Tim Harris, Harvey Meyer, Georg von Hippel, Jonas Wilhelm, and Hartmut Wittig, "Nucleon charges and quark momentum fraction with $N_f = 2 + 1$ Wilson fermions," PoS **LATTICE2018**, 129 (2018), arXiv:1809.10638 [hep-lat].

[72] G. S. Bali, S. Collins, M. Gruber, A. Schfer, P. Wein, and T. Wurm (RQCD), "Solving the PCAC puzzle for nucleon axial and pseudoscalar form factors," Phys. Lett. **B789**, 666–674 (2019), arXiv:1810.05569 [hep-lat].

[73] Eigo Shintani, Ken-Ichi Ishikawa, Yoshinobu Kuramashi, Shoichi Sasaki, and Takeshi Yamazaki (PACS), "Nucleon form factors and root-mean-square radii on a $(10.8\ \mathrm{fm})^4$ lattice at the physical point," Phys. Rev. **D99**, 014510 (2019), arXiv:1811.07292 [hep-lat].

[74] Martha Constantinou, Constantia Alexandrou, Simone Bacchio, Kyriakos Hadjiyiannakou, Karl Jansen, Giannis Koutsou, and Alejandro Vaquero Aviles-Casco, "Nucleon form factors from $N_f = 2 + 1 + 1$ twisted-mass fermions at the physical point," PoS **LATTICE2018**, 142 (2018).

[75] Yong-Chull Jang, Tanmoy Bhattacharya, Rajan Gupta, Huey-Wen Lin, and Boram Yoon (PNDME), "Updates on nucleon form factors from clover-on-HISQ lattice formulation," PoS **LATTICE2018**, 123 (2018), arXiv:1901.00060 [hep-lat].

[76] Veronique Bernard, Latifa Elouadrhiri, and Ulf-G. Meissner, "Axial structure of the nucleon," J. Phys. **G28**, R1–R35 (2002), arXiv:hep-ph/0107088 [hep-ph].

[77] Rajan Gupta, Yong-Chull Jang, Boram Yoon, Huey-Wen Lin, Vincenzo Cirigliano, and Tanmoy Bhattacharya (PNDME), "Isovector charges of the nucleon from 2+1+1-flavor lattice

QCD," Phys. Rev. **D98**, 034503 (2018), arXiv:1806.09006 [hep-lat].

[78] S. Aoki *et al.* (Flavor Lattice Averaging Group), "Review of lattice results concerning low-energy particle physics," Eur. Phys. J. **C77**, 112 (2017), arXiv:1607.00299 [hep-lat]; "FLAG review 2019," arXiv:1902.08191 [hep-lat]; updates can be found on the FLAG website.

[79] Tanmoy Bhattacharya, Vincenzo Cirigliano, Saul Cohen, Rajan Gupta, Anosh Joseph, Huey-Wen Lin, and Boram Yoon (PNDME), "Isovector and isoscalar tensor charges of the nucleon from lattice QCD," Phys. Rev. **D92**, 094511 (2015), arXiv:1506.06411 [hep-lat].

[80] S. Arzumanov, L. Bondarenko, S. Chernyavsky, P. Geltenbort, V. Morozov, V. V. Nesvizhevsky, Yu. Panin, and A. Strepetov, "A measurement of the neutron lifetime using the method of storage of ultracold neutrons and detection of inelastically up-scattered neutrons," Phys. Lett. **B745**, 79–89 (2015).

[81] A. T. Yue, M. S. Dewey, D. M. Gilliam, G. L. Greene, A. B. Laptev, J. S. Nico, W. M. Snow, and F. E. Wietfeldt, "Improved determination of the neutron lifetime," Phys. Rev. Lett. **111**, 222501 (2013), arXiv:1309.2623 [nucl-ex].

[82] Aaron S. Meyer, Richard J. Hill, Andreas S. Kronfeld, Ruizi Li, and James N. Simone, "Calculation of the nucleon axial form factor using staggered lattice QCD," PoS **LATTICE2016**, 179 (2016), arXiv:1610.04593 [hep-lat].

[83] N. N. Meiman, "Analytic expressions for upper limits of coupling constants in quantum field theory," Sov. Phys. JETP **17**, 830 (1963), [Zh. Eksp. Teor. Fiz. **44**, 1228 (1963)].

[84] Richard J. Hill and Gil Paz, "Model independent extraction of the proton charge radius from electron scattering," Phys. Rev. **D82**, 113005 (2010), arXiv:1008.4619 [hep-ph].

[85] Richard J. Hill, "The modern description of semileptonic meson form factors," eConf **C060409**, 027 (2006), arXiv:hep-ph/0606023 [hep-ph].

[86] C. Bernard *et al.* (Fermilab Lattice, MILC), "The $\bar{B} \to D^* \ell \bar{\nu}$ form factor at zero recoil from three-flavor lattice QCD: A model-independent determination of $|V_{cb}|$," Phys. Rev. **D79**, 014506 (2009), arXiv:0808.2519 [hep-lat].

[87] Jon A. Bailey *et al.* (Fermilab Lattice, MILC), "The $B \to \pi \ell \nu$ semileptonic form factor from three-flavor lattice QCD: A model-independent determination of $|V_{ub}|$," Phys. Rev. **D79**, 054507 (2009), arXiv:0811.3640 [hep-lat].

[88] Andr de Gouva and Kevin J. Kelly, "Non-standard neutrino interactions at DUNE," Nucl. Phys. **B908**, 318–335 (2016), arXiv:1511.05562 [hep-ph].

[89] Julian Heeck, Manfred Lindner, Werner Rodejohann, and Stefan Vogl, "Non-standard neutrino interactions and neutral gauge bosons," (2018), arXiv:1812.04067 [hep-ph].

[90] D. S. Armstrong and R. D. McKeown, "Parity-violating electron scattering and the electric and magnetic strange form factors of the nucleon," Annu. Rev. Nucl. Part. Sci. **62**, 337–359 (2012), arXiv:1207.5238 [nucl-ex].

[91] Zhihong Ye, John Arrington, Richard J. Hill, and Gabriel Lee, "Proton and neutron electromagnetic form factors and uncertainties," Phys. Lett. **B777**, 8–15 (2018), arXiv:1707.09063 [nucl-ex].

[92] Raza Sabbir Sufian, "Neutral weak form factors of proton and neutron," Phys. Rev. **D96**, 093007 (2017), arXiv:1611.07031 [hep-ph].

[93] G. Garvey, E. Kolbe, K. Langanke, and S. Krewald, "Role of strange quarks in quasielastic neutrino scattering," Phys. Rev. **C48**, 1919–1925 (1993).

[94] G. T. Garvey, W. C. Louis, and D. H. White, "Determination of proton strange form-factors from νp elastic scattering," Phys. Rev. **C48**, 761–765 (1993).

[95] A. A. Aguilar-Arevalo *et al.* (MiniBooNE), "Measurement of the neutrino neutral-current elastic differential cross section on mineral oil at $E_\nu \sim 1$ GeV," Phys. Rev. **D82**, 092005 (2010), arXiv:1007.4730 [hep-ex].

[96] A. A. Aguilar-Arevalo *et al.* (MiniBooNE), "Measurement of the antineutrino neutral-current elastic differential cross section," Phys. Rev. **D91**, 012004 (2015), arXiv:1309.7257 [hep-ex].

[97] A. Fatima, M. Sajjad Athar, and S. K. Singh, "Second class currents and T violation in quasielastic neutrino and antineutrino scattering from nucleons," Phys. Rev. **D98**, 033005 (2018), arXiv:1806.08597 [hep-ph].

[98] Huey-Wen Lin, "Hyperon physics from lattice QCD," Nucl. Phys. Proc. Suppl. **187**, 200–207 (2009), arXiv:0812.0411 [hep-lat].

[99] Shoichi Sasaki, "Status of semileptonic hyperon decays from lattice QCD using 2+1 flavor domain wall fermions," PoS **LATTICE2013**, 388 (2014).

[100] G. P. Zeller *et al.* (NuTeV), "A precise determination of electroweak parameters in neutrino nucleon scattering," Phys. Rev. Lett. **88**, 091802 (2002), **90**, 239902E (2003), arXiv:hep-ex/0110059 [hep-ex].

[101] J. T. Londergan and Anthony William Thomas, "Charge symmetry violation corrections to determination of the Weinberg angle in neutrino reactions," Phys. Rev. **D67**, 111901 (2003), arXiv:hep-ph/0303155 [hep-ph].

[102] Yong Ding, Rong-Guang Xu, and Bo-Qiang Ma, "Effect of asymmetric strange-antistrange sea to the NuTeV anomaly," Phys. Lett. **B607**, 101–106 (2005), arXiv:hep-ph/0408292 [hep-ph].

[103] M. Gluck, P. Jimenez-Delgado, and E. Reya, "Radiatively generated isospin violations in the nucleon and the NuTeV anomaly," Phys. Rev. Lett. **95**, 022002 (2005), arXiv:hep-ph/0503103 [hep-ph].

[104] K. J. Eskola and H. Paukkunen, "NuTeV $\sin^2\theta_w$ anomaly and nuclear parton distributions revisited," JHEP **06**, 008 (2006), arXiv:hep-ph/0603155 [hep-ph].

[105] I. C. Cloet, W. Bentz, and A. W. Thomas, "Isovector EMC effect explains the NuTeV anomaly," Phys. Rev. Lett. **102**, 252301 (2009), arXiv:0901.3559 [nucl-th].

[106] W. Bentz, I. C. Cloet, J. T. Londergan, and A. W. Thomas, "Reassessment of the NuTeV determination of the weak mixing angle," Phys. Lett. **B693**, 462–466 (2010), arXiv:0908.3198 [nucl-th].

[107] S. Davidson, S. Forte, P. Gambino, N. Rius, and A. Strumia, "Old and new physics interpretations of the NuTeV anomaly," JHEP **02**, 037 (2002), arXiv:hep-ph/0112302 [hep-ph].

[108] Stefan Kretzer, Fredrick Olness, Jon Pumplin, Daniel Stump, Wu-Ki Tung, and Mary Hall Reno, "The parton structure of the nucleon and precision determination of the Weinberg angle in neutrino scattering," Phys. Rev. Lett. **93**, 041802 (2004), arXiv:hep-ph/0312322 [hep-ph].

[109] H. L. Lai, Pavel M. Nadolsky, J. Pumplin, D. Stump, W. K. Tung, and C.-P. Yuan, "The strange parton distribution of the nucleon: Global analysis and applications," JHEP **04**, 089 (2007), arXiv:hep-ph/0702268 [hep-ph].

[110] David Alexander Mason, *Measurement of the strange-antistrange asymmetry at NLO in QCD from NuTeV dimuon data*, Ph.D. thesis, University of Oregon (2006).

[111] Derek B. Leinweber, Terrence Draper, and R. M. Woloshyn, "Baryon octet to decuplet electromagnetic transitions," Phys. Rev. **D48**, 2230–2249 (1993), arXiv:hep-lat/9212016 [hep-lat].

[112] C. Alexandrou, G. Koutsou, H. Neff, John W. Negele, W. Schroers, and A. Tsapalis, "Nucleon to Δ electromagnetic transition form factors in lattice QCD," Phys. Rev. **D77**, 085012 (2008), arXiv:0710.4621 [hep-lat].

[113] C. Alexandrou, G. Koutsou, Th. Leontiou, John W. Negele, and A. Tsapalis, "Axial nucleon and nucleon to Δ form factors and the Goldberger-Treiman relations from lattice QCD," Phys. Rev. **D76**, 094511 (2007), [**D80**, 099901 (2009)], arXiv:0706.3011 [hep-lat].

[114] A. A. Aguilar-Arevalo *et al.* (MiniBooNE), "Significant excess of electron-like events in the MiniBooNE short-baseline neutrino experiment," Phys. Rev. Lett. **121**, 221801 (2018), arXiv:1805.12028 [hep-ex].

[115] M. Lüscher, "Volume dependence of the energy spectrum in massive quantum field theories 2: Scattering states," Commun. Math. Phys. **105**, 153–188 (1986); "Two particle states on a torus and their relation to the scattering matrix," Nucl. Phys. **B354**, 531–578 (1991).

[116] Laurent Lellouch and Martin Lüscher, "Weak transition matrix elements from finite volume correlation functions," Commun. Math. Phys. **219**, 31–44 (2001), arXiv:hep-lat/0003023 [hep-lat].

[117] S. Aoki *et al.* (CP-PACS), "Lattice QCD calculation of the ρ meson decay width," Phys. Rev. **D76**, 094506 (2007), arXiv:0708.3705 [hep-lat].

[118] Xu Feng, Karl Jansen, and Dru B. Renner, "Resonance parameters of the rho-meson from lattice QCD," Phys. Rev. **D83**, 094505 (2011), arXiv:1011.5288 [hep-lat].

[119] Jozef J. Dudek, Robert G. Edwards, and Christopher E. Thomas (Hadron Spectrum), "Energy dependence of the ρ resonance in $\pi\pi$ elastic scattering from lattice QCD," Phys. Rev. **D87**, 034505 (2013), [Erratum: Phys. Rev.D90,no.9,099902(2014)], arXiv:1212.0830 [hep-ph].

[120] David J. Wilson, Ral A. Briceo, Jozef J. Dudek, Robert G. Edwards, and Christopher E. Thomas, "Coupled $\pi\pi, K\bar{K}$ scattering in P-wave and the ρ resonance from lattice QCD," Phys. Rev. **D92**, 094502 (2015), arXiv:1507.02599 [hep-ph].

[121] Constantia Alexandrou, Luka Leskovec, Stefan Meinel, John Negele, Srijit Paul, Marcus Petschlies, Andrew Pochinsky, Gumaro Rendon, and Sergey Syritsyn, "P-wave $\pi\pi$ scattering and the ρ resonance from lattice QCD," Phys. Rev. **D96**, 034525 (2017), arXiv:1704.05439 [hep-lat].

[122] Silas R. Beane, Thomas C. Luu, Kostas Orginos, Assumpta Parreno, Martin J. Savage, Aaron Torok, and Andre Walker-Loud, "Precise Determination of the I=2 pi pi Scattering Length from Mixed-Action Lattice QCD," Phys. Rev. **D77**, 014505 (2008), arXiv:0706.3026 [hep-lat].

[123] Xu Feng, Karl Jansen, and Dru B. Renner, "The $\pi^+\pi^+$ scattering length from maximally twisted mass lattice QCD," Phys. Lett. **B684**, 268–274 (2010), arXiv:0909.3255 [hep-lat].

[124] S. R. Beane, E. Chang, W. Detmold, H. W. Lin, T. C. Luu, K. Orginos, A. Parreno, M. J. Savage, A. Torok, and A. Walker-Loud (NPLQCD), "The $I = 2$ $\pi\pi$ s-wave scattering phase shift from lattice QCD," Phys. Rev. **D85**, 034505 (2012), arXiv:1107.5023 [hep-lat].

[125] Jozef J. Dudek, Robert G. Edwards, Michael J. Peardon, David G. Richards, and Christopher E. Thomas, "The phase-shift of isospin-2 π-π scattering from lattice QCD," Phys. Rev. **D83**, 071504 (2011), arXiv:1011.6352 [hep-ph].

[126] Jozef J. Dudek, Robert G. Edwards, and Christopher E. Thomas, "S and D-wave phase shifts in isospin-2 $\pi\pi$ scattering from lattice QCD," Phys. Rev. **D86**, 034031 (2012), arXiv:1203.6041 [hep-ph].

[127] William Detmold and Martin J. Savage, "Electroweak matrix elements in the two nucleon sector from lattice QCD," Nucl. Phys. **A743**, 170–193 (2004), arXiv:hep-lat/0403005 [hep-

lat].
[128] Song He, Xu Feng, and Chuan Liu, "Two particle states and the S-matrix elements in multi-channel scattering," JHEP **07**, 011 (2005), arXiv:hep-lat/0504019 [hep-lat].
[129] Maxwell T. Hansen and Stephen R. Sharpe, "Multiple-channel generalization of Lellouch-Lüscher formula," Phys. Rev. **D86**, 016007 (2012), arXiv:1204.0826 [hep-lat].
[130] Ral A. Briceo and Zohreh Davoudi, "Moving multichannel systems in a finite volume with application to proton-proton fusion," Phys. Rev. **D88**, 094507 (2013), arXiv:1204.1110 [hep-lat].
[131] Peng Guo, Jozef Dudek, Robert Edwards, and Adam P. Szczepaniak, "Coupled-channel scattering on a torus," Phys. Rev. **D88**, 014501 (2013), arXiv:1211.0929 [hep-lat].
[132] Simon Kreuzer and H.-W. Hammer, "The triton in a finite volume," Phys. Lett. **B694**, 424–429 (2011), arXiv:1008.4499 [hep-lat].
[133] Ral A. Briceo and Zohreh Davoudi, "Three-particle scattering amplitudes from a finite volume formalism," Phys. Rev. **D87**, 094507 (2013), arXiv:1212.3398 [hep-lat].
[134] Ulf-G. Meiner, Guillermo Ros, and Akaki Rusetsky, "Spectrum of three-body bound states in a finite volume," Phys. Rev. Lett. **114**, 091602 (2015), [Erratum: Phys. Rev. Lett.117,no.6,069902(2016)], arXiv:1412.4969 [hep-lat].
[135] Ral A. Briceo, Maxwell T. Hansen, and Stephen R. Sharpe, "Relating the finite-volume spectrum and the two-and-three-particle S matrix for relativistic systems of identical scalar particles," Phys. Rev. **D95**, 074510 (2017), arXiv:1701.07465 [hep-lat].
[136] Ral A. Briceo, Maxwell T. Hansen, and Stephen R. Sharpe, "Three-particle systems with resonant subprocesses in a finite volume," Phys. Rev. **D99**, 014516 (2019), arXiv:1810.01429 [hep-lat].
[137] M. Dring, H.-W. Hammer, M. Mai, J.-Y. Pang, A. Rusetsky, and J. Wu, "Three-body spectrum in a finite volume: the role of cubic symmetry," Phys. Rev. **D97**, 114508 (2018), arXiv:1802.03362 [hep-lat].
[138] Silas R. Beane, William Detmold, Thomas C. Luu, Kostas Orginos, Martin J. Savage, and Aaron Torok, "Multi-pion systems in lattice QCD and the three-pion interaction," Phys. Rev. Lett. **100**, 082004 (2008), arXiv:0710.1827 [hep-lat].
[139] Jozef J. Dudek, Robert G. Edwards, and David J. Wilson (Hadron Spectrum), "An a_0 resonance in strongly coupled $\pi\eta$, $K\bar{K}$ scattering from lattice QCD," Phys. Rev. **D93**, 094506 (2016), arXiv:1602.05122 [hep-ph].
[140] Ral A. Briceo, Jozef J. Dudek, Robert G. Edwards, and David J. Wilson (Hadron Spectrum), "Isoscalar $\pi\pi$, $K\bar{K}$, $\eta\eta$ scattering and the σ, f_0, f_2 mesons from QCD," Phys. Rev. **D97**, 054513 (2018), arXiv:1708.06667 [hep-lat].
[141] Antoni Woss, Christopher E. Thomas, Jozef J. Dudek, Robert G. Edwards, and David J. Wilson (Hadron Spectrum), "Dynamically-coupled partial-waves in $\rho\pi$ isospin-2 scattering from lattice QCD," JHEP **07**, 043 (2018), arXiv:1802.05580 [hep-lat].
[142] Ral A. Briceo and Maxwell T. Hansen, "Multichannel $0 \to 2$ and $1 \to 2$ transition amplitudes for arbitrary spin particles in a finite volume," Phys. Rev. **D92**, 074509 (2015), arXiv:1502.04314 [hep-lat].
[143] Ral A. Briceo, Jozef J. Dudek, Robert G. Edwards, Christian J. Shultz, Christopher E. Thomas, and David J. Wilson, "The $\pi\pi \to \pi\gamma^\star$ amplitude and the resonant $\rho \to \pi\gamma^\star$ transition from lattice QCD," Phys. Rev. **D93**, 114508 (2016), arXiv:1604.03530 [hep-ph].
[144] Constantia Alexandrou, Luka Leskovec, Stefan Meinel, John Negele, Srijit Paul, Marcus Petschlies, Andrew Pochinsky, Gumaro Rendon, and Sergey Syritsyn, "$\pi\gamma \to \pi\pi$ transi-

tion and the ρ radiative decay width from lattice QCD," Phys. Rev. **D98**, 074502 (2018), arXiv:1807.08357 [hep-lat].

[145] Ral A. Briceo and Maxwell T. Hansen, "Relativistic, model-independent, multichannel $2 \to 2$ transition amplitudes in a finite volume," Phys. Rev. **D94**, 013008 (2016), arXiv:1509.08507 [hep-lat].

[146] Alessandro Baroni, Ral A. Briceo, Maxwell T. Hansen, and Felipe G. Ortega-Gama, "Form factors of two-hadron states from a covariant finite-volume formalism," (2018), arXiv:1812.10504 [hep-lat].

[147] Christian W. Andersen, John Bulava, Ben Hrz, and Colin Morningstar, "Elastic $I = 3/2$ P-wave nucleon-pion scattering amplitude and the $\Delta(1232)$ resonance from $N_f = 2+1$ lattice QCD," Phys. Rev. **D97**, 014506 (2018), arXiv:1710.01557 [hep-lat].

[148] Noemi Rocco, Alessandro Lovato, and Omar Benhar, "Unified description of electron-nucleus scattering within the spectral function formalism," Phys. Rev. Lett. **116**, 192501 (2016), arXiv:1512.07426 [nucl-th].

[149] Keh-Fei Liu and Shao-Jing Dong, "Origin of difference between $\bar{d}$ and $\bar{u}$ partons in the nucleon," Phys. Rev. Lett. **72**, 1790–1793 (1994), arXiv:hep-ph/9306299 [hep-ph].

[150] K. F. Liu, S. J. Dong, Terrence Draper, D. Leinweber, J. H. Sloan, W. Wilcox, and R. M. Woloshyn, "Valence QCD: connecting QCD to the quark model," Phys. Rev. **D59**, 112001 (1999), arXiv:hep-ph/9806491 [hep-ph].

[151] Keh-Fei Liu, "Parton degrees of freedom from the path-integral formalism," Phys. Rev. **D62**, 074501 (2000), arXiv:hep-ph/9910306 [hep-ph].

[152] U. Aglietti, Marco Ciuchini, G. Corbo, E. Franco, G. Martinelli, and L. Silvestrini, "Model independent determination of the shape function for inclusive b decays and of the structure functions in DIS," Phys. Lett. **B432**, 411–420 (1998), arXiv:hep-ph/9804416 [hep-ph].

[153] William Detmold and C. J. David Lin, "Deep-inelastic scattering and the operator product expansion in lattice QCD," Phys. Rev. **D73**, 014501 (2006), arXiv:hep-lat/0507007 [hep-lat].

[154] Keh-Fei Liu, "Parton distribution function from the hadronic tensor on the lattice," PoS **LATTICE2015**, 115 (2016), arXiv:1603.07352 [hep-ph].

[155] A. J. Chambers, R. Horsley, Y. Nakamura, H. Perlt, P. E. L. Rakow, G. Schierholz, A. Schiller, K. Somfleth, R. D. Young, and J. M. Zanotti (QCDSF), "Nucleon structure functions from operator product expansion on the lattice," Phys. Rev. Lett. **118**, 242001 (2017), arXiv:1703.01153 [hep-lat].

[156] Maxwell T. Hansen, Harvey B. Meyer, and Daniel Robaina, "From deep inelastic scattering to heavy-flavor semileptonic decays: Total rates into multihadron final states from lattice QCD," Phys. Rev. **D96**, 094513 (2017), arXiv:1704.08993 [hep-lat].

[157] Jian Liang, Keh-Fei Liu, and Yi-Bo Yang, "Lattice calculation of hadronic tensor of the nucleon," EPJ Web Conf. **175**, 14014 (2018), arXiv:1710.11145 [hep-lat].

[158] Xiangdong Ji, "Parton physics on a Euclidean lattice," Phys. Rev. Lett. **110**, 262002 (2013), arXiv:1305.1539 [hep-ph].

[159] Giancarlo Rossi and Massimo Testa, "Euclidean versus Minkowski short distance," Phys. Rev. **D98**, 054028 (2018), arXiv:1806.00808 [hep-lat].

[160] Krzysztof Cichy and Martha Constantinou, "A guide to light-cone PDFs from lattice QCD: an overview of approaches, techniques and results," (2018), arXiv:1811.07248 [hep-lat].

[161] Christopher Monahan, "Recent developments in x-dependent structure calculations," PoS **LATTICE2018**, 018 (2018), arXiv:1811.00678 [hep-lat].

[162] Huey-Wen Lin, Jiunn-Wei Chen, Saul D. Cohen, and Xiangdong Ji, "Flavor structure of the nucleon sea from lattice QCD," Phys. Rev. **D91**, 054510 (2015), arXiv:1402.1462 [hep-ph].
[163] A. V. Radyushkin, "Quasi-parton distribution functions, momentum distributions, and pseudo-parton distribution functions," Phys. Rev. **D96**, 034025 (2017), arXiv:1705.01488 [hep-ph].
[164] Yan-Qing Ma and Jian-Wei Qiu, "Exploring partonic structure of hadrons using *ab initio* lattice QCD calculations," Phys. Rev. Lett. **120**, 022003 (2018), arXiv:1709.03018 [hep-ph].
[165] Jiunn-Wei Chen, Luchang Jin, Huey-Wen Lin, Yu-Sheng Liu, Andreas Schfer, Yi-Bo Yang, Jian-Hui Zhang, and Yong Zhao (LP^3), "First direct lattice-QCD calculation of the x-dependence of the pion parton distribution function," (2018), arXiv:1804.01483 [hep-lat].
[166] Ral A. Briceo, Juan V. Guerrero, Maxwell T. Hansen, and Christopher J. Monahan, "Finite-volume effects due to spatially nonlocal operators," Phys. Rev. **D98**, 014511 (2018), arXiv:1805.01034 [hep-lat].
[167] Gunnar S. Bali, Bernhard Lang, Bernhard U. Musch, and Andreas Schfer, "Novel quark smearing for hadrons with high momenta in lattice QCD," Phys. Rev. **D93**, 094515 (2016), arXiv:1602.05525 [hep-lat].
[168] B. Buck and S. M. Perez, "New look at magnetic moments and beta decays of mirror nuclei," Phys. Rev. Lett. **50**, 1975–1978 (1983).
[169] D. Krofcheck *et al.*, "Gamow-Teller strength function in ^{71}Ge via the (p, n) reaction at medium-energies," Phys. Rev. Lett. **55**, 1051–1054 (1985).
[170] W. T. Chou, E. K. Warburton, and B. Alex Brown, "Gamow-Teller beta-decay rates for $A \leq 18$ nuclei," Phys. Rev. **C47**, 163–177 (1993).
[171] A. Baroni, L. Girlanda, S. Pastore, R. Schiavilla, and M. Viviani, "Nuclear axial currents in chiral effective field theory," Phys. Rev. **C93**, 015501 (2016), [Erratum: Phys. Rev.C95,no.5,059901(2017)], arXiv:1509.07039 [nucl-th].
[172] H. Krebs, E. Epelbaum, and U. G. Meiner, "Nuclear axial current operators to fourth order in chiral effective field theory," Ann. Phys. **378**, 317–395 (2017), arXiv:1610.03569 [nucl-th].
[173] S. Pastore, A. Baroni, J. Carlson, S. Gandolfi, Steven C. Pieper, R. Schiavilla, and R. B. Wiringa, "Quantum Monte Carlo calculations of weak transitions in $A = 6$-10 nuclei," Phys. Rev. **C97**, 022501 (2018), arXiv:1709.03592 [nucl-th].
[174] A. Lovato, S. Gandolfi, J. Carlson, Steven C. Pieper, and R. Schiavilla, "Electromagnetic and neutral-weak response functions of ^{4}He and ^{12}C," Phys. Rev. **C91**, 062501 (2015), arXiv:1501.01981 [nucl-th].
[175] A. Lovato, S. Gandolfi, J. Carlson, Ewing Lusk, Steven C. Pieper, and R. Schiavilla, "Quantum Monte Carlo calculation of neutral-current ν-^{12}C inclusive quasielastic scattering," Phys. Rev. **C97**, 022502 (2018), arXiv:1711.02047 [nucl-th].
[176] Martin J. Savage, Phiala E. Shanahan, Brian C. Tiburzi, Michael L. Wagman, Frank Winter, Silas R. Beane, Emmanuel Chang, Zohreh Davoudi, William Detmold, and Kostas Orginos (NPLQCD), "Proton-proton fusion and tritium β decay from lattice quantum chromodynamics," Phys. Rev. Lett. **119**, 062002 (2017), arXiv:1610.04545 [hep-lat].
[177] Emmanuel Chang, Zohreh Davoudi, William Detmold, Arjun S. Gambhir, Kostas Orginos, Martin J. Savage, Phiala E. Shanahan, Michael L. Wagman, and Frank Winter (NPLQCD), "Scalar, axial, and tensor interactions of light nuclei from lattice QCD," Phys. Rev. Lett. **120**, 152002 (2018), arXiv:1712.03221 [hep-lat].
[178] Brian C. Tiburzi, Michael L. Wagman, Frank Winter, Emmanuel Chang, Zohreh Davoudi, William Detmold, Kostas Orginos, Martin J. Savage, and Phiala E. Shanahan, "Double-β

decay matrix elements from lattice quantum chromodynamics," Phys. Rev. **D96**, 054505 (2017), arXiv:1702.02929 [hep-lat].

[179] N. Barnea, L. Contessi, D. Gazit, F. Pederiva, and U. van Kolck, "Effective field theory for lattice nuclei," Phys. Rev. Lett. **114**, 052501 (2015), arXiv:1311.4966 [nucl-th].

[180] A. Bansal, S. Binder, A. Ekstrm, G. Hagen, G. R. Jansen, and T. Papenbrock, "Pionless effective field theory for atomic nuclei and lattice nuclei," Phys. Rev. **C98**, 054301 (2018), arXiv:1712.10246 [nucl-th].

[181] L. Contessi, A. Lovato, F. Pederiva, A. Roggero, J. Kirscher, and U. van Kolck, "Ground-state properties of ^{4}He and ^{16}O extrapolated from lattice QCD with pionless EFT," Phys. Lett. **B772**, 839–848 (2017), arXiv:1701.06516 [nucl-th].

[182] Johannes Kirscher, Ehoud Pazy, Jonathan Drachman, and Nir Barnea, "Electromagnetic characteristics of $A \leq 3$ physical and lattice nuclei," Phys. Rev. **C96**, 024001 (2017), arXiv:1702.07268 [nucl-th].

[183] Alessandro Roggero and Joseph Carlson, "Linear response on a quantum computer," (2018), arXiv:1804.01505 [quant-ph].

[184] William Detmold and Michael G. Endres, "Signal/noise enhancement strategies for stochastically estimated correlation functions," Phys. Rev. **D90**, 034503 (2014), arXiv:1404.6816 [hep-lat].

[185] Silas R. Beane, William Detmold, Kostas Orginos, and Martin J. Savage, "Uncertainty quantification in lattice QCD calculations for nuclear physics," J. Phys. **G42**, 034022 (2015), arXiv:1410.2937 [nucl-th].

[186] Michael L. Wagman and Martin J. Savage, "Taming the signal-to-noise problem in lattice QCD by phase reweighting," (2017), arXiv:1704.07356 [hep-lat].

[187] Michael L. Wagman and Martin J. Savage, "Statistics of baryon correlation functions in lattice QCD," Phys. Rev. **D96**, 114508 (2017), arXiv:1611.07643 [hep-lat].

[188] William Detmold, Gurtej Kanwar, and Michael L. Wagman, "Phase unwrapping and one-dimensional sign problems," Phys. Rev. **D98**, 074511 (2018), arXiv:1806.01832 [hep-lat].